ACS APPLIED MATERIALS & INTERFACES

Review

Cite This: ACS Appl. Mater. Interfaces 2019, 11, 6685−6704

www.acsami.org

Recent Advances in Flexible and Wearable Pressure Sensors Based on Piezoresistive 3D Monolithic Conductive Sponges

Yichun Ding,[†] Tao Xu,[†] Obiora Onyilagha,[‡] Hao Fong,[†,‡,§] and Zhengtao Zhu*[,†,‡,§]

[†]Biomedical Engineering Ph.D. Program, [‡]Nanoscience and Nanoengineering Ph.D. Program, [§]Department of Chemistry and Applied Biological Sciences, South Dakota School of Mines & Technology, Rapid City, South Dakota 57701, United States

ABSTRACT: High-performance flexible strain and pressure sensors are important components of the systems for human motion detection, human−machine interaction, soft robotics, electronic skin, etc., which are envisioned as the key technologies for applications in future human healthcare monitoring and artificial intelligence. In recent years, highly flexible and wearable strain/pressure sensors have been developed based on various materials/structures and transduction mechanisms. Piezoresistive three-dimensional (3D) monolithic conductive sponge, the resistance of which changes upon external pressure or stimuli, has emerged as a forefront material for flexible and wearable pressure sensor due to its excellent sensor performance, facile fabrication, and simple circuit integration. This review focuses on the rapid development of the piezoresistive pressure sensors based on 3D conductive sponges. Various piezoresistive conductive sponges are categorized into four different types and their material and structural characteristics are summarized. Methods for preparation of the 3D conductive sponges are reviewed, followed by examples of device performance and selected applications. The review concludes with a critical reflection of the current status and challenges. Prospects of the 3D conductive sponge for flexible and wearable pressure sensor are discussed.

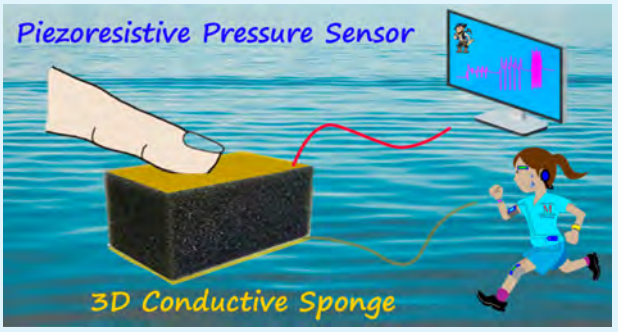

KEYWORDS: *wearable electronics, piezoresistive pressure sensor, conductive sponge, human motion monitoring, electronic skin*

1. INTRODUCTION

Flexible and wearable sensors for monitoring human health and activities have attracted tremendous attention in recent years.[1−6] The commercially available wearable gadgets such as Fitbit wristband and Apple watch can track physical activities and physiological signals for daily fitness,[5] but these devices are hardly considered as flexible and wearable systems. It is still a great challenge to develop "true" flexible/wearable sensor systems with integrated merits of multifunctionality, high sensitivity, fast response, low-cost, and more importantly, conformability with human skin/body and soft materials (such as textile).[7−9]

A strain/pressure sensor, which detects the signal variation in response to mechanical deformation or external stimuli, is an important device for applications in human motion detection, human−machine interaction, soft robotics, artificial electronic skin, etc.[10−17] For human motion monitoring, the strain/pressure sensor is required to be highly sensitive over a wide detection range from subtle motions (e.g., speaking, heartbeat, and wrist pulse) to vigorous movement (e.g., joint bending, muscle movements, and walking).[17−21] In recent years, novel materials and/or structures composed of soft polymers and nanomaterials have been investigated as flexible strain and pressure sensors for detection of large strain.[6,22−25] These strain/pressure sensors convert mechanical force and/or deformation into electrical signal; the transduction mechanisms include piezoresistivity, capacitance, piezoelectricity, and triboelectricity.[15,18,26,27] The capacitive pressure sensor measures the capacitance change of a capacitor with a deformable dielectric material sandwiched between two flexible conductive plates under applied pressure.[28−30] The capacitance of the device is determined by $C = \varepsilon A/d$, where C is the capacitance, ε is the dielectric constant of the dielectric layer material, A is the overlap area of the two electrodes, and d is the thickness of the dielectric layer.[17] Upon compression, the thickness of the deformable dielectric layer changes, leading to the change of the capacitance. The capacitive pressure sensor has high sensitivity in detection of static deformation and also has low power consumption, but it usually has limited detection range of strain.[16] The piezoelectric and triboelectric pressure sensors are based on the piezoelectric and triboelectric effects of materials (e.g., ZnO, $BaTiO_3$, and PVDF).[26,31−33] The most significant advantage of these sensors is that they can be operated with low power consumption or even without external power supply (i.e., self-powered pressure sensors).[26] However, these sensors can only detect transient/dynamic deformation because of the intermittence nature of piezoelectric and triboelectric effects. Additionally, fabrication of these sensors typically requires complicated micropatterning and delicate packaging processes. The piezoresistive sensor

Received: November 28, 2018
Accepted: January 28, 2019
Published: January 28, 2019

DOI: 10.1021/acsami.8b20929
ACS Appl. Mater. Interfaces 2019, 11, 6685−6704

transduces the external pressure into a resistance signal. Conductive elastomeric composites or conductive porous sponges have been investigated for flexible and wearable piezoresistive pressure sensors, which show the capability of detection of the high strain changes during human motions.[19,34−36] Under the compressive force, the temporary contact areas/points of the porous conductive sponge increase to form more conductive pathways, which lead to decrease of the resistance.[17] Moreover, the number of temporary contacts is determined by the strain/pressure of compression; therefore, the piezoresistive pressure sensor can detect both transient and static deformation. These piezoresistive sensors have the advantages of simple fabrication, low cost, easy signal acquisition, fast response, and wide detection range.[37−40] Number of publications in materials, processing, and devices for flexible piezoresistive sensors has increased rapidly in recent years, as shown in Figure 1. Several review articles are available in the field of flexible and wearable strain/pressure sensors.[17,23−25,41]

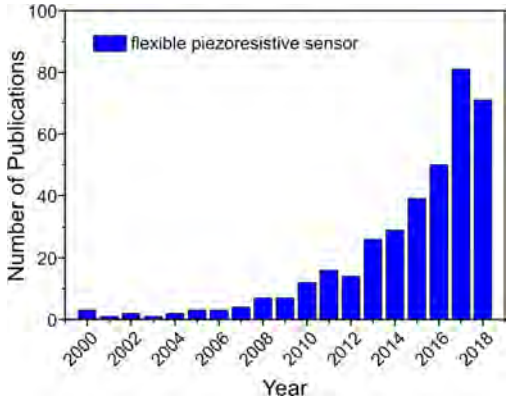

Figure 1. Number of publications with the topic of "flexible piezoresistive sensor" indexed in the Web of Science from year 2000 to October 2018.

The conventional piezoresistive strain/pressure sensors are based on single-crystal silicon, metals, metal oxide films, and nitride materials; these devices are highly sensitive but have very limited flexibility and range of strain (typically less than ~1%) because of the intrinsic rigid and brittle nature of the inorganic materials.[42,43] Several innovative material/structure strategies have been developed for flexible/stretchable piezoresistive strain/pressure sensors. Rogers and Huang groups pioneered the structural design of stretchable electronics/devices based on inorganic materials (e.g., single crystalline silicon, III−V semiconductor, and metal thin film). Assembly of micro/nanostructures of inorganic semiconductors on strained elastomer/flexible substrates enables stretchable electronics/sensors through mechanics-guided and deterministic buckling; stretchable interconnects, which are important for stretchable/flexible products for real-world application, can be designed on the basis of the serpentine/fractal-inspired patterning of metal films (e.g., Au, indium tin oxide).[44−47] In another approach, two flexible/stretchable electrodes with patterned pyramid, dome, porous, or pre-strained wavy microstructures are assembled into piezoresistive strain/pressure sensor, in which the resistance change under applied pressure is correlated with the contacts between the two electrodes.[48−53] The two strategies discussed above not only require patterning and fabrication processes of micro/nanostructures but also have relatively limited detection range of strains. Recently, three-dimensional (3D) and porous conductive materials have emerged as promising materials for flexible piezoresistive strain/pressure sensors. These 3D spongy structures have advantageous features of lightweight, large strain range, simple device fabrication, and low cost, etc. Additionally, assembly of functional soft materials and nanomaterials (e.g., carbon nanotubes, conducting polymers, metal nanostructures) into 3D spongy structures are of fundamental interests to the material scientists and engineers, and may have various applications such as electrode materials in electrochemical energy storage devices. Herein, this review aims to give a comprehensive survey of the 3D monolithic conductive sponges for piezoresistive pressure sensors. The conductive sponges are first categorized into various types and the characteristic features of each type are summarized. Second, methods and processes for preparation of 3D conductive sponges are discussed. Pressure sensors based on conductive sponges, as well as their potential applications in human motion monitoring, are demonstrated using selective examples. The review concludes with outlook of the remaining challenges and future perspectives in the field.

2. TYPES OF 3D CONDUCTIVE SPONGES FOR PRESSURE SENSORS

Excellent mechanical elasticity, high compressibility, and good conductivity are essential requirements for material that may be used in wearable/flexible pressure sensor. Many materials and methods have been reported in the past few years to prepare 3D conductive sponges for wearable/flexible pressure sensors. Conductive materials such as carbon nanotubes (CNTs), graphene, metal nanowires, and conducting polymers are common building blocks to construct 3D conductive sponges by innovative assembly processes;[54−57] well-established spongy materials are also shown as good templates for preparation of 3D conductive sponges.[19,58−60] As shown in Figure 2, the 3D conductive sponges can be categorized into four types based on their structures and compositions: (1) neat conductive sponge, (2) composite conductive sponge, (3) conductive sponge impregnated with elastomer, and (4) conductive material coated sponge. Each type has its own characteristics; the details are discussed below.

2.1. Neat Conductive Sponge. Neat conductive sponge refers to the 3D porous spongy structure assembled from the conductive material only. Carbon materials such as carbon nanotubes (CNTs), graphene, and graphene oxide, owing to their excellent mechanical, electrical, and thermal properties, are the most popular building blocks for construction of neat 3D conductive sponges with high conductivity and ultralow density. 3D spongy structures of CNTs and/or graphene can be directly fabricated by the method of catalyzed chemical vapor deposition (CVD) or freeze-drying assembly.[37,54,55,75] Since CNTs have one-dimensional structure and graphene has two-dimensional sheet structure, they can be properly self-assembled into 3D interconnected networks, forming robust monolithic conductive sponges. Similarly, metal nanowires (e.g., Cu nanowires)[56] and conducting polymers (e.g., polypyrrole, PPy)[57] can also be processed into 3D structures by the freeze-drying method. In addition, neat conductive sponges can be prepared by carbonization of polymer sponges, cellulose-assembled sponges, and wood materials.[63,76,77] Although the neat conductive sponges have ultralow densities, high conductivity, and good thermal and chemical stability,

DOI: 10.1021/acsami.8b20929
ACS Appl. Mater. Interfaces 2019, 11, 6685−6704

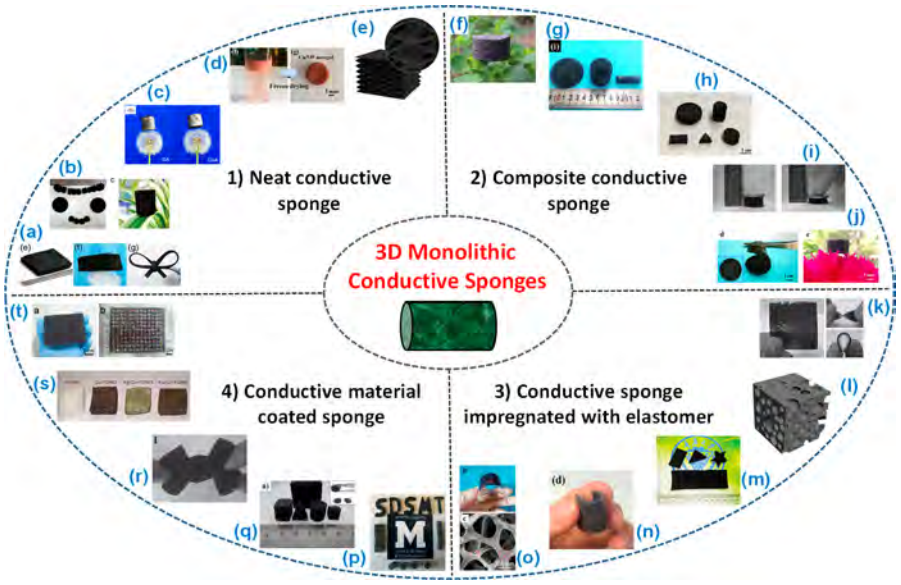

Figure 2. Various types of 3D monolithic conductive sponges for fabrication of piezoresistive pressure sensors. (1) Neat conductive sponge: (a) Flexible carbon nanotubes (CNTs) foam prepared by CVD. Reprinted with permission from ref 54. Copyright 2017 John Wiley and Sons. (b) Zn_2GeO_4@PPy nanowire aerogel. Reprinted with permission from ref 61. Copyright 2017 Royal Society of Chemistry. (c) Ultralight graphene aerogel. Reprinted with permission from ref 62. Copyright 2017 Elsevier. (d) Copper nanowire aerogel. Reprinted with permission from ref 56. Copyright 2017 American Chemical Society. (e) Compressible carbon sponge derived from natural wood. Reprinted with permission from ref 63. Copyright 2018 Elsevier. (2) Polymer/conductive material composite sponges: (f) Graphene/TPU composite foam. Reprinted with permission from ref 34. Copyright 2017 Royal Society of Chemistry. (g) CNTs/TPU/epoxy composite sponge. Reprinted with permission from ref 64. Copyright 2017 Elsevier. (h) 3D nanofibrous PAN/PI/CNFs composite sponge. Reprinted with permission from ref 65. Copyright 2017 Royal Society of Chemistry. (i) CNTs/PI composite sponge, Reprinted with permission from ref 66 Copyright 2017 John Wiley and Sons. (j) CNT/TPU composite foam. Reprinted with permission from ref 67. Copyright 2017 American Chemical Society. (3) Conductive sponge impregnated with elastomer: (k) 3D PPy@graphene sponge filled with PDMS. Reprinted with permission from ref.68. Copyright 2016 John Wiley and Sons. (l) MOF-derived porous carbon/PDMS composite. Reprinted with permission from ref.69. Copyright 2018 American Chemical Society. (m) Carbonized sponge filled with silicone resin. Reprinted with permission from ref 66. Copyright 2017 Royal Society of Chemistry. (n) 3D graphene sponge filled with PDMS. Reprinted with permission from ref 70. Copyright 2016 American Chemical Society. (o) 3D CNTs/graphene sponge filled with PDMS. Reprinted with permission from ref 71. Copyright 2017 John Wiley and Sons. (4) Conductive material coated sponge: (p) PEDOT:PSS@Melamine sponge. Reprinted with permission from ref 19. Copyright 2018 American Chemical Society. (q) Graphene@PU sponge. Reprinted with permission from ref 72. Copyright 2017 Royal Society of Chemistry. (r) Carbon black@PU sponge. Reprinted with permission from ref 58. Copyright 2016 John Wiley and Sons. (s) Metal (Cu, Ag/Cu, Au/Cu)-coated PDMS sponge. Reprinted with permission from ref 73. Copyright 2016 John Wiley and Sons. (t) Graphene@PU sponge. Reprinted with permission from ref 74. Copyright 2013 John Wiley and Sons.

these materials may have limited sensitivity and range of compressive strain because of their intrinsic mechanically rigid and fragile nature. The network structures of these neat conductive sponges can be easily subjected to irreversible damage during compression, causing plastic deformations and severe/irreversible changes in the electrical conductivity. To overcome this drawback, the neat conductive sponge can be impregnated with an elastic polymer, which is referred as the conductive sponge impregnated with elastomer (section 2.3).

2.2. Composite Conductive Sponge. Composite conductive sponge refers to the sponge composed of blends of polymer and conductive material. Composite conductive sponge is prepared by adding polymer binder during the assembly of conductive material or mixing the conductive material and polymer components, followed by methods such as foaming or freeze-drying.[78] For example, Liu et al.[34] prepared porous graphene/thermoplastic polyurethane (TPU) foam with tunable conductivity by freeze-drying; Xu and Ding et al.[65] reported a 3D conductive sponge prepared by the assembly of shortened electrospun nanofibers of polyacrylonitrile (PAN), polyimide (PI), and PAN-based carbon nanofibers (CNFs). In composite conductive sponge, the conductivity and sensitivity are readily tuned by varying the amount of the conductive component. One intractable issue of the composite conductive sponge is the nonuniform dispersion of the conductive material and/or polymer during the fabrication. In addition, the hysteresis effect and irreversible plastic deformation due to the intrinsic plastic behavior of the polymer component may be problematic for the composite conductive sponge.[34,64,67] Surface functionalization of conductive material to improve the dispersion in polymer and design of composite structures with multicomponents are important to mitigate the hysteresis and improve the long-term stability.[79,80]

2.3. Conductive Sponge Impregnated with Elastomer. Conductive sponge impregnated with elastomer refers to the spongy structure that the neat conductive sponge is infiltrated/coated with elastic polymer to strengthen the stability and compressibility of the sponge.[66,70,81,82] The elastic polymer such as TPU, silicone, or polydimethylsiloxane (PDMS) is coated on the framework of the neat conductive sponge with a thin layer; thus the highly porous structure can be maintained. The conductive sponge coated by elastomer possesses good compression stability and relatively good reproducibility of electrical resistance change during cyclic compression. Additionally, if the conductive sponge is fully infiltrated with elastomer (i.e., embedded in elastomer), it might be highly stretchable and can be used as stretchable

DOI: 10.1021/acsami.8b20929
ACS Appl. Mater. Interfaces 2019, 11, 6685−6704

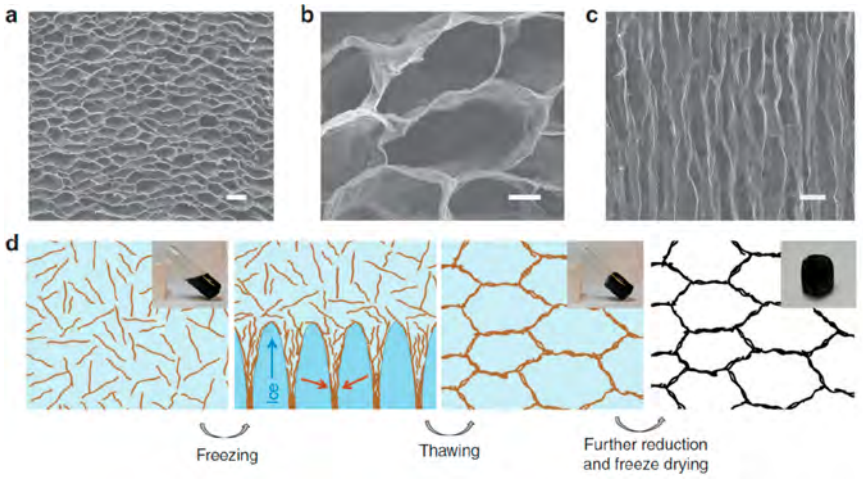

Figure 3. Morphology and formation mechanism of the cork-like graphene elastomer. (a–c) Typica (a, b)l top-view and (c) side-view SEM images of graphene monolith. (d) Schematic showing the formation mechanism of the cork-like monolith by freeze casting. Photos of the corresponding samples are presented in the insets. Scale bars: (a, c) 50 and (b) 10 μm. Reprinted with permission from ref 55. Copyright 2012 Nature Publishing Group.

strain sensor.[83−85] The drawback of the conductive sponge impregnated with polymer is a significant decrease of conductivity and increase of density. Better control of the amount and thickness of the coated polymer layer during preparation would be helpful to prepare the conductive sponge impregnated with polymer with desired electric and mechanical properties. Vapor or in situ polymerization/deposition may help to achieve good and uniform coating of polymer layers on the conductive sponge.

2.4. Conductive Material-Coated Sponge. Conductive material coated sponge refers to the conductive sponge composed of nonconductive polymer sponge coated with the conductive material by methods such as sputtering, dip coating, and in situ polymerization.[19,59,86] For example, a thin layer of metal nanoparticles or film can be deposited on the 3D framework of a sponge by ionic sputtering or wet-chemical deposition (ion-exchange method).[59,87] Nonconductive polymer sponge can also be made conductive by direct dip coating in a solution or dispersion of carbon and metals.[88−90] Issues with carbon or metals (i.e., CNTs, graphene, Ag, etc.) as conductive coating include the sophisticated and costly preparation processes, formation of a unstable and non-homogeneous "ink" for dip coating, and the poor adhesion between conductive material and the sponge.[91] Conducting polymers (e.g., PPy, PANI, PEDOT:PSS) are soft and flexible with high electrical conductivity and good adhesive property; they are considered as excellent conductive materials or synergistic enhancing components for conductive material-coated sponge.[19,86,92−94]

3. METHODS FOR FABRICATION OF 3D CONDUCTIVE SPONGE

As mentioned above, the 3D conductive sponge can be made from neat conductive material, conductive material/polymer composite, or a 3D structure comprising a scaffold component and a conductive component. Methods such as self-gelation have been used for fabrication of conductive sponges/aerogels (e.g., CNTs and graphene sponges/aerogels) in the past;[54,95−97] these 3D conductive sponges/aerogels have attracted diverse applications in oil−water separation, oil absorption, flexible conductor, and energy storage/conversion devices due to their lightweight, hydrophobic behavior, porous hierarchical structure, and unique electrical properties, etc.[54,97,98] However, the brittle nature and plastic deformation under strain/stress fail these materials in applications for flexible/wearable strain/pressure sensor.[99] Innovative methods have to be developed in preparation of the spongy conductive material with robust and elastic mechanical properties under strain/pressure.[100,101] These methods can be broadly categorized as assembly of nanomaterials by freezing-drying and template sponge-based assembly/synthesis. We discuss these novel methods for construction of various 3D conductive sponges in details.

3.1. Freeze-Drying Method. Freeze-drying, technically known as lyophilization, is a dehydration process in which the frozen water (or solvent) in the material sublimes directly from the solid phase to the gas phase under reduced pressure. During the freezing step, the dispersed building block materials (e.g., polymer, and shortened nanofibers) are concentrated and entrapped at the boundaries of the solvent crystals. As the crystals grow, these building block materials are eventually locked into a 3D solid network due to the expansion of the crystals. In the subsequent drying step, the solidified solvent sublimes, and a 3D porous structure/sponge is obtained. The structure of this 3D sponge is a replica of the polycrystalline morphology of the solidified solvent. The pore structure and pore size/size distribution can be adjusted by the freeze-drying processing conditions (e.g., solvent system, freezing rate, freezing direction, and drying speed).[102] Notably, by controlling the direction of the freezing (i.e., directional freeze-drying), a uniformly ordered and/or aligned porous structure can be obtained.[64]

3.1.1. Freezing-Drying for the Conductive Sponge. Freezing-drying of the conductive material has been used to prepare neat conductive sponge such as flexible and elastic graphene sponge.[37,103] In a typical process, graphene oxide (GO) is used as the raw material. The GO is dispersed in a solvent to form a suspension or a hydrogel by adding additives;[35,40,62,75] subsequently, freezing and freeze-drying processes are performed to obtain the 3D structure by removing the water/solvent under reduced pressure. The reduction of GO to the reduced graphene oxide (rGO) is achieved either by chemical/hydrothermal reduction during the solution process or by high-temperature annealing reduction after formation of the 3D structure.[35,40,62,75] By using the freeze-drying method, the density of the obtained sponge can be adjusted by controlling the amount/concentration of GO; and the shape and pore structure can also be readily tailored by the freeze-drying conditions such as mold shape/size and freezing direction, rate, and time.

Figure 3 shows the mechanism of the freeze-drying preparation of a superelastic graphene-based monolith that could be compressed up to 80% strain and fully recovered after compression.[55] The 3D graphene sponge was prepared from partially reduced GO (pr-GO) by using a

DOI: 10.1021/acsami.8b20929
ACS Appl. Mater. Interfaces 2019, 11, 6685−6704

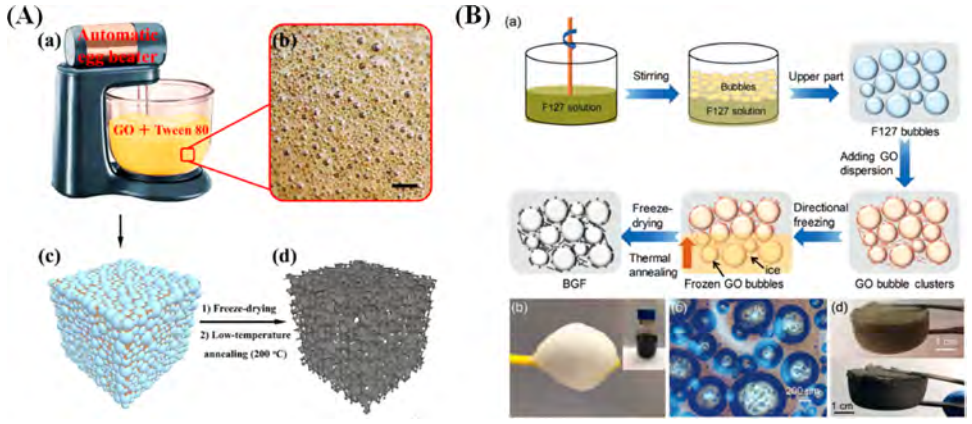

Figure 4. (A) Illustrations for the preparation of sparkling graphene block (SGB): (a) 50 mL of GO dispersion (5 mg mL^{-1}) and 7 mL of TWEEN 80 (100 mg mL^{-1}, dissolved in ethanol) mixed under stirring using an automatic egg beater at 1300 rpm for 10 min, (b) enlarged view of the gas bubbles in the mixture (scale bar, 1 mm), (c) homogeneous mixture of air bubbles and GO, and (d) SGB obtained after freeze-drying and heated at 200 °C. Reprinted with permission from ref 38. Copyright 2017 American Chemical Society. (B) Schematic illustration of the assembly strategy of bubble-derived graphene foams (BGFs):(a) schematic illustration of the assembly strategy of BGFs, including the bubbling of the F127 solution by vigorous stirring, collecting of bubble clusters, adding of GO dispersion, directional freezing, freeze-drying, and thermal annealing, (b) photograph of F127 bubble clusters, with low density and flowability. The inset shows a bottle of GO dispersion with the concentration of 5 mg mL^{-1}, (c) optical microscope image of the GO bubbles with the stirring rate of 250 rpm, (d) photographs of the bubble-derived GO foam and BGF-5 obtained after thermal annealing. Reprinted with permission from ref 27. Copyright 2018 John Wiley and Sons.

multistep freeze-casting process (i.e., freezing, thawing, dialysis, freeze-drying, and thermal annealing reduction). As shown in Figure 3a–c, the 3D graphene monolith showed a cellular/honeycomb-like network structure. Figure 3d illustrates the fabrication process and formation mechanism. When the pr-GO dispersion was frozen, the pr-GO sheets were concentrated at the boundary of ice crystals and then aligned along the growth direction of ice due to the squeezing effect. After the ice was thawed, a pr-GO network was formed; the network retained its connectivity followed by subsequent thermal annealing. The use of pr-GO was key to obtaining the highly elastic sponge. The $\pi-\pi$ attraction between the pr-GO sheets was enhanced as a result of partial reduction; therefore, the as-formed network was quite stable and could maintain its structural integrity upon thawing.[55]

A synergistic strategy is developed to fabricate conductive sponge with enhanced elasticity by integrating multiple conductive materials (e.g., CNTs, graphene, MXene).[104−106] For example, Lv et al.[105] prepared CNTs-enhanced 3D graphene sponge by introducing CNTs into graphene through hydrothermal reduction and freeze-drying. In this CNTs-enhanced graphene structure, the CNTs entangled and covered the graphene sheets, which prevented the sliding between the graphene sheets, enhanced the stiffness of cell walls, and provided the aerogel with superelasticity. Mechanical test showed that the graphene/CNT aerogel could fully recover without fracture even after 90% compression.

The graphene conductive sponge can also be formed by combination of freeze-drying with traditional foaming and blowing process by introducing gas bubbles using sonication, shearing, and sparkling agent/surfactant.[100,38,107,108] As shown in Figure 4A, Lv et al.[38] used an automatic egg beater to stir a GO suspension with sparkling agent (TWEEN 80) to generate a large number of micron-sized air bubbles (100−300 μm) during stirring. Thereafter, a 3D compressive rGO sponge (sparkling graphene block, SGB) was obtained by freeze-drying and thermal reduction. The SGB exhibited an excellent elasticity even at 95% compressive strain, and the as-fabricated pressure sensor showed an ultrahigh pressure sensitivity of 229.8 kPa^{-1}. In Figure 4B, Zhang et al.[27] prepared a graphene sponge by a strategy of combining bubbling and ice templating. Air bubble clusters were first generated by stirring a surfactant solution, then the GO suspension was mixed with the bubbles. The 3D graphene sponge was obtained by subsequent freeze-drying and thermal reduction processes. However, this bubble-derived GO sponge showed 3% plastic deformation at 50% strain during cyclic compression; infiltration of PDMS to the sponge was needed to fabricate a stable pressure sensor.

Besides the carbon materials, conducting polymers and metal nanowires can be assembled into 3D neat conductive sponge by the freeze-drying method. Lv et al. reported a 3D porous PPy sponge prepared by freeze-drying.[57] One disadvantage of the resulting 3D PPy sponge was the relatively poor mechanical elasticity; it might be improved through rationally designed strategies such as stepwise growth procedure[57] or adding another component (e.g., metal nanowires) as a framework.[61] Similarly, metal nanowires could form 3D conductive hydrogel;[56] during the hydrogel process, the one-dimensional nanowires with large aspect ratio were accumulated, entrapped, and interconnected with each other, leading to a robust self-assembled sponge after the freeze-drying process.[56]

3.1.2. Freeze-Drying for Preparation of Conductive Composite Sponge. It is well-known that the polymer is softer and more flexible than the carbon and metal materials. Therefore, polymer is used to enhance the plasticity/elasticity of the 3D conductive sponge either by mixing with the conductive material to form a composite sponge or by infiltrating into conductive sponge.[109] Conventionally, the direct blending of elastic polymer with conductive material only forms very dense or slightly porous bulky material, which has limited compressibility.[110] Recently, by adopting the freeze-drying process, highly porous and hierarchically structured conductive composite sponges have been prepared. For example, Liu et al.[34] prepared highly porous lightweight conductive graphene/TPU foam by mixing graphene with TPU solution followed by freeze-drying. The graphene/TPU foam showed ultralow density of about 0.11 g cm^{-3} and porosity of 90%; the material demonstrated good compressibility and stable piezoresistive sensing response at a strain of up to 90%. Moreover, the conductivity and sensitivity of the graphene/TPU foam could be tuned by adjusting the amount of graphene in the composite sponge.

Directional-freezing method can be applied to assemble 3D conductive sponge with hierarchical pore structure and aligned channels. For example, a CNTs/TPU conductive sponge with aligned porous structure and a CNTs/TPU/epoxy sponge with herringbone-like structure were fabricated by directional-freezing method.[64,67] The aligned porous structure and herringbone-like structure could significantly improve the compression reversibility of the resulting sponges. However, these polymer composite sponges showed some extent of plastic deformation and needed a precompression process to improve the piezoresistive stability. To further improve the elastic

DOI: 10.1021/acsami.8b20929
ACS Appl. Mater. Interfaces 2019, 11, 6685−6704

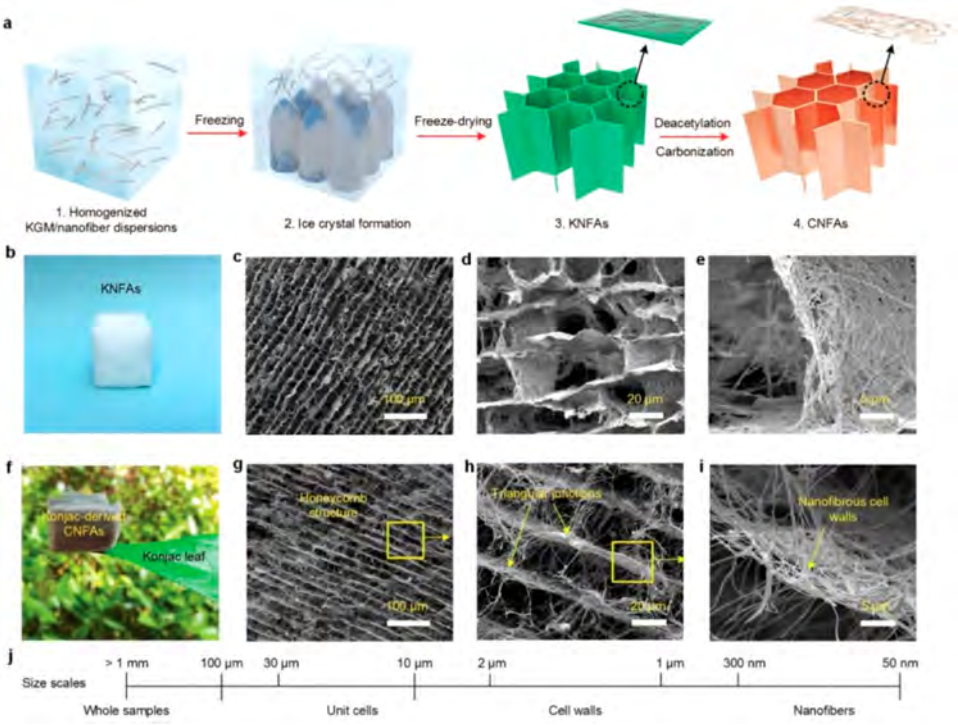

Figure 5. (a) Schematic showing the synthetic steps. (b) Optical photograph of a KGM/SiO_2 nanofiber composite aerogel (KNFA). (c–e) Microscopic structure of KNFAs at different magnifications. (f) Optical photograph showing a 20 cm^3 carbonaceous nanofibrous aerogel (CNFA) (ρ = 0.14 mg cm^{-3}) standing on the tip of a konjac leaf. (g–i) Microscopic structure of CNFAs at various magnifications, demonstrating the biomimetic honeycomb cellular fibrous architecture. (j) Schematic showing the four levels of hierarchy at three distinct length scales. Reprinted with permission from ref 122. Copyright 2016 John Wiley and Sons.

property of the 3D conductive sponge, a polymer with good mechanical property can be used in the composite sponge. For example, polyimide (PI), a class of outstanding engineering polymers with excellent mechanical properties, thermal stability, and chemical resistance,[111] has been used to fabricate 3D composite sponge with superelasticity, good compressibility, and stability.[66,82,112] Besides various synthetic polymers, cellulose or bacterial cellulose nanofibers are other promising building materials for constructing conductive sponge by freeze-drying because of their nanofibrous structure and abundant/sustainable plant-based source.[113,114]

3.1.3. Freeze-Drying Assembly of Electrospun Nanofibers. Freeze-drying assembly of shortened electrospun nanofibers to form 3D porous sponge has stimulated broad research interests recently. Ultralight sponges have been prepared from various electrospun nanofibers of polymer, ceramic and carbon by freeze-drying.[115−121] Compared to CNTs, graphene, metal nanowires, and conducting polymers, the electrospun nanofibers have significant advantages of easy fabrication, ultrahigh aspect ratio, variety of structures, and flexibility, *etc*. In a typical process for fabrication of 3D sponge, short nanofibers or small pieces of nanofibers, obtained by shortening/homogenizing the as-electrospun nanofibers, are first dispersed in a solvent with added binders to form a slurry/suspension; subsequently, the slurry/suspension is shaped to a desired size by freezing in a mold, and finally, the 3D nanofibrous sponge is obtained by freeze-drying under reduced pressure. For example, Si et al.[122] reported an ultralight, biomass-derived carbonaceous nanofibrous aerogel with superelasticity and high pressure-sensitivity. As illustrated in Figure 5, electrospun SiO_2 nanofibers were homogenized and dispersed in water to form a homogeneous dispersion with the addition of konjac glucomannan (KGM, a biomass). The dispersion was frozen by liquid nitrogen, during which ice crystals were formed. Next, a 3D KGM/SiO_2 nanofiber composite aerogel (KNFA) was obtained by freeze-drying. Finally, carbonaceous nanofibrous aerogels (CNFA) was produced through high-temperature carbonization of KNFA. The resulting CNFA exhibited robust mechanical properties under large elastic deformations (80% compressive strain).

In another example, Xu and Ding et al.[65] reported freeze-drying of multicomponent electrospun nanofibers to prepare a 3D conductive sponge for pressure sensor application. The 3D conductive sponge was prepared by assembly of shortened electrospun nanofibers of PAN, PI, and CNFs, in which the PAN and PI nanofibers served as the scaffold component and the CNFs served as the conductive component. This 3D nanofibrous conductive sponge showed tunable conductivity and sensitivity by varying the content of the carbon nanofibers; pressure sensor fabricated by the 3D conductive sponge demonstrated high sensitivity and stability.

3.2. Template Sponge-Based Assembly and Synthesis. Template method is widely used to prepare nanomaterials and 3D porous materials. In the template sponge-based assembly and synthesis of conductive sponge, 3D and porous sponge material such as commercially available melamine-formaldehyde (MF) sponge is typically used as a template, and various methods and conductive materials can be developed and incorporated during assembly and synthesis processes.

3.2.1. Carbonization of Template Sponge. High-temperature pyrolysis or carbonization is the most straightforward method to produce carbon material. However, most polymer materials are largely decomposed with very low carbon yield during the high-temperature pyrolysis; for example, the widely used PAN has a carbon yield of about 40 wt % when used as a precursor for producing carbon fiber by pyrolysis.[123] Furthermore, the high volume/structure shrinkage during carbonization typically results in rigid and brittle carbon material. Therefore, it is difficult to prepare carbon sponge by carbonization of the template polymer sponge. One exception is the MF sponge. Because of its high nitrogen content and 3D open-cell network structure, MF sponge can be carbonized to form elastic carbon sponge.[124,125] Recently, MF-derived elastic carbon sponge has been used for compressible pressure sensor application.[66,76,126] Carbon sponge with high compressibility could also be prepared by

DOI: 10.1021/acsami.8b20929
ACS Appl. Mater. Interfaces 2019, 11, 6685−6704

carbonization of bacterial cellulose assembled-sponge;[77] however, a laminated carbon composite prepared by carbonization of nano-lignocellulose/graphene composite only had very limited range of recoverable compression strain (<3%).[127] Sponge formed by adding small amount (0.5−1.5 wt %) of cellulose nanocrystalline in rGO followed by high-temperature carbonization was reported to have supercompressibility (undergoing an extreme strain of 99%) and elasticity (100% height retention after 10,000 cycles at a strain of 30%).[128] Such superior mechanical property was attributed to the enhanced interactions between rGO layers by incorporating the low-molecular-weight carbon precursor (cellulose nanocrystalline). Recently, Zhao et al.[69] reported porous carbon sponge derived from carbonization of metal−organic framework (MOF); the MOF-derived porous carbon embedded in PDMS was demonstrated as wearable pressure and temperature sensor.

Natural wood is an abundant and sustainable resource; it is generally not highly compressible. Song et al.[129] developed a method to prepare a highly compressible wood (up to 60% strain) by removal of the lignin and hemicellulose components from bulk wood, which partially destroyed the thin cell walls of wood and left layered structure with aligned cellulose nanofibers. Such highly compressible wood could be carbonized to compressible wood carbon sponge (WCS), as shown in Figure 6. The WCS from the treated wood was highly compressible (80% strain), suitable for piezoresistive pressure sensor, while the carbon wood from pristine wood was very brittle.[63]

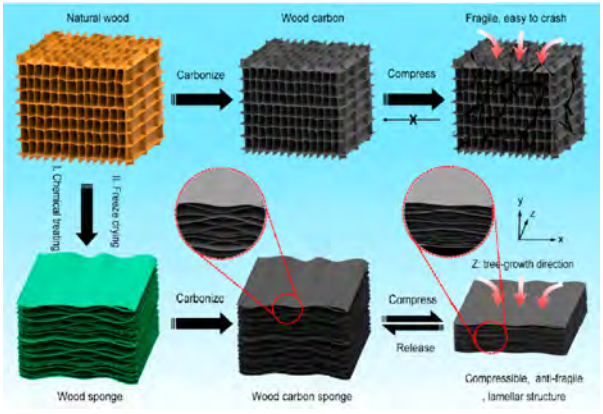

Figure 6. Graphical illustration of the design and fabrication process of the fragile wood carbon (WC) and the highly compressible wood carbon sponge (WCS). As a result of the unique arched layered structure, the WCS has anisotropic mechanical properties and is highly compressible. Reprinted with permission from ref 63. Copyright 2018 Elsevier.

3.2.2. Template Removal Methods. Sacrificial template method is widely used to prepare porous structure, in which the sacrificial template material serves as a temporary framework in assisting the formation of desired 3D structure.[130−132] The sacrificial template can then be decomposed, dissolved, or etched after the formation of the 3D conductive sponge.

Template Removal by Decomposition. Polymer sponge that can be completely decomposed is a good candidate for preparation of conductive sponge by the template removal method. Samad et al.[133] prepared a graphene sponge by using commercial PU foam as a sacrificial template. As shown in Figure 7, the PU foam was first dip coated with GO, and the GO-coated PU was heat-treated at 1000 °C in nitrogen atmosphere. During the pyrolysis of the GO-coated-PU, GO was reduced to graphene foam, whereas the PU was simultaneously decomposed and completely released as volatiles. The overall shrinkage during the pyrolysis was about 12%. The obtained rGO sponge was later filled with PDMS and used as a pressure sensor.

Template Removal by Etching. Metal foam such as nickel (Ni) and copper (Cu) can be used for synthesis of monolithic graphene

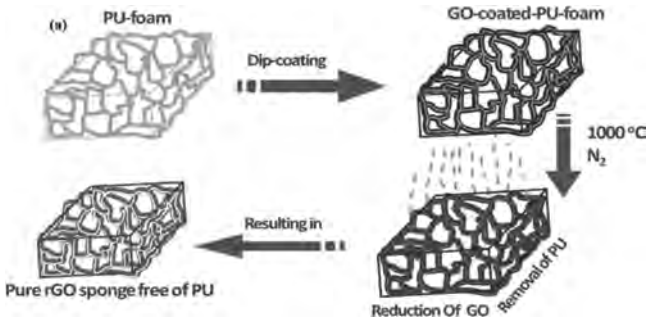

Figure 7. Schematic representation of graphene foam preparation by polyurethane sponge template. Reprinted with permission from ref 133. Copyright 2015 John Wiley and Sons.

foam (sponge) by CVD method, in which the metal foam serves not only as the framework but also as the catalyst.[83−85,134] An example of this method is shown in Figure 8a.[70] Graphene was grown directly on the framework of a cleaned Ni (or Cu) foam by CVD; after growth of graphene, the Ni (or Cu) foam was etched by chemical solution to obtain a freestanding graphene foam.[70,71,81,134] However, such a freestanding neat graphene sponge had relatively poor mechanical strength against compression; therefore, for the compressible pressure sensor application, a layer of polymer (e.g., PDMS) was coated or infiltrated on the graphene@Ni (or Cu) foam before etching away the metal foam.[55,70] Similar method was also used to prepare a 3D freestanding conducting polymer foam.[68] As shown in Figure 8b, first, PPy is coated on the Ni foam by electrochemical deposition; then by etching away the Ni foam using 1 M $FeCl_3$ solution, a freestanding PPy foam was obtained. This freestanding PPy foam was used as a strain sensor after infiltration with PDMS.

Template Removal by Dissolution. Porous and dissolvable material, such as sugar cube, is a good sacrificial template for preparation of porous sponge since the template material can be removed simply by dissolution in a solvent. Various flexible and compressible PDMS sponges have been fabricated by the sugar template method for stretchable electrode applications.[101,135,136] 3D conductive sponge can also be prepared using the sugar template by incorporating a conductive component during sponge preparation or by dip coating in conductive inks after sponge preparation.[90,136,137] Figure 9 shows an example of using sugar template to prepare a conductive sponge of CNT@PDMS.[90] A commercial sugar cube was first used as a sacrificial template to prepare a microporous PDMS (pPDMS) sponge by infiltrating PDMS prepolymer followed by dissolving the sugar template. Subsequently, the replica pPDMS sponge was drop-casted with CNT ink to prepare a conductive sponge. The commercial MF could be used as the sacrificial skeleton to prepare a superelastic and arbitrary-shaped graphene aerogel by the template dissolution removal method;[138] after the formation of the 3D graphene aerogel, the MF sponge was removed by dissolution in hydroiodic acid solution.

3.2.3. Surface Coating of a Template Sponge. The surface coating strategy based on a readily available sponge is a simple, straightforward, and efficient way to prepare conductive sponge. Commercially available polymer sponge (e.g., TPU, MF) or as-fabricated sponge can be deposited with a layer of conductive material. Such conductive sponge generally maintains the good elasticity of the pristine polymer sponge. Key to this process is to achieving good adhesion between the template sponge and the conductive coating material, which is essential to ensure stability and reproducibility of the conductive spongy material/device.

Sputter Coating on a Template Sponge. Metal and carbon materials can be deposited on a polymer sponge through methods such as ion sputtering and physical vapor deposition (PVD). A thin layer of metal/carbon film coated on the framework of the sponge can make the sponge highly conductive. One challenge is that the sputtered/deposited metal or carbon layer forms cracks easily during compression owing to the intrinsic rigid nature of metal/carbon. For

DOI: 10.1021/acsami.8b20929
ACS Appl. Mater. Interfaces 2019, 11, 6685−6704

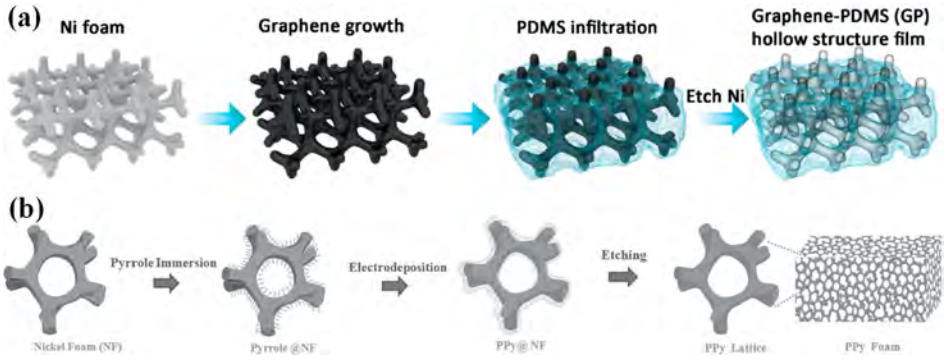

Figure 8. (a) Fabrication process of hollow-structured graphene–PDMS (GP) composite. Reprinted with permission from ref 81. Copyright 2017 John Wiley and Sons. (b) Illustration of the fabrication process for the fabrication of 3D PPy foam. Reprinted with permission from ref 68. Copyright 2016 John Wiley and Sons.

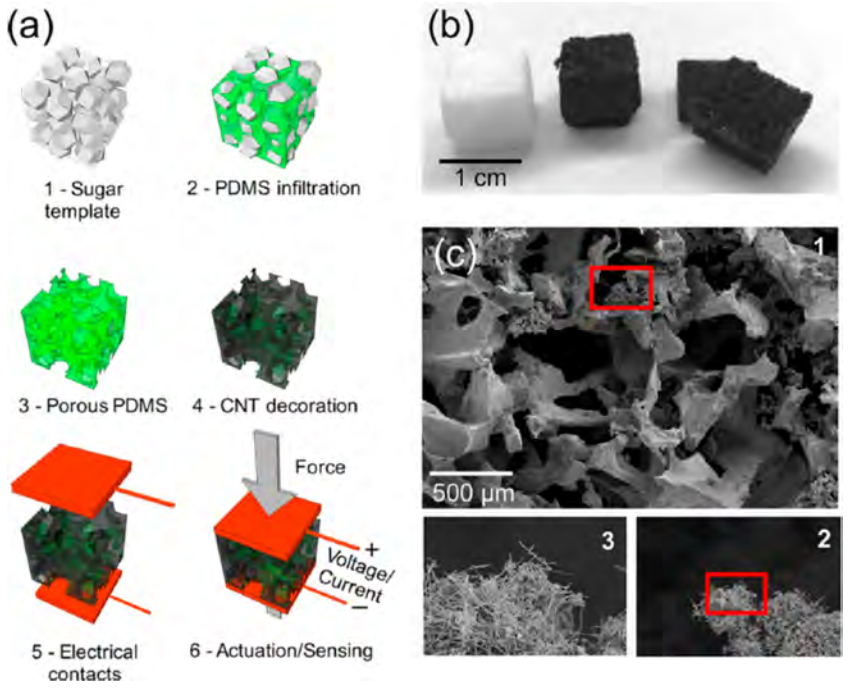

Figure 9. Preparation and morphological characterization of pPDMS/CNT foams: (a) Preparation steps of macroporous PDMS (pPDMS) foams and decoration with CNTs. (b) Optical pictures of pPDMS foams with 500 ± 300 μm pores (larger pore foams) before (white) and after (black) CNT decoration (both full-size and cross-section). (c) Scanning electron microscope (SEM) images of the cross-section of a pPDMS/CNT foam with 500 ± 300 μm pores and CNT density of 25 mg cm^{-3} at different magnifications. Reprinted with permission from ref 90. Copyright 2018 American Chemical Society.

example, Wu et al.[59] prepared a gold-coated PU sponge (Au@PU) by ion sputtering; the Au@PU formed channel cracks when compressed. Such channel cracks led to increase of resistance at relatively low compression strain (<20%); and the resistance of the Au@PU pressure sensor decreased at higher strains (>20%) due to the "contact effect".

Dip Coating/Drop Casting on a Template Sponge. Dip coating, drop casting, or soaking is a simple and scalable method in preparation of surface coated material, which is similar to the industrial dyeing process. Various "inks" including suspensions of carbon materials (e.g., carbon black (CB), CNTs, graphene),[72,74,88,90,91,137,139−141] metal nanoparticles/nanowires,[39,89,142] conducting polymers,[19,92] MXene,[143] or their hybrids[39,60,89,144] have been used to prepare the conductive sponge by this method. The conductive material is commonly coated on the sponge framework through physical forces (e.g., electrostatic force, $\pi-\pi$ interaction). Because of its two-dimensional sheet structure, graphene may be wrapped on the sponge skeleton, resulting in relatively good adhesion. Major challenges in the dip coating/drop casting of conductive "ink" on a template sponge include the instability and nonuniformity of the conductive inks and the poor adhesion between the conductive coating material and the template due to the weak physical interactions. Aggregation of carbon or metal nanomaterials in suspension may be problematic in formulating a stable and homogeneous "ink" and for coating the template sponge uniformly. Additionally, the CB and metal nanoparticles are easily cracked and peeled off from a sponge when adhesion is poor. To achieve uniform and strong conductive coating on a template sponge, the wettability of the sponge and the conductive component needs to be carefully considered. In this case, conducting polymer may be a good choice as the conductive ink for uniform dip coating and formation of good adhesion because of the soft nature and homogeneous dispersion of the material.[19] Recently, other novel conductive materials, such as ionic liquid or tungsten disulfide (WS_2) nanosheets, have been explored for preparation of conductive sponge.[145,146] The ionic liquid provides good wetting process and has flexible properties;[145] WS_2

DOI: 10.1021/acsami.8b20929
ACS Appl. Mater. Interfaces 2019, 11, 6685−6704

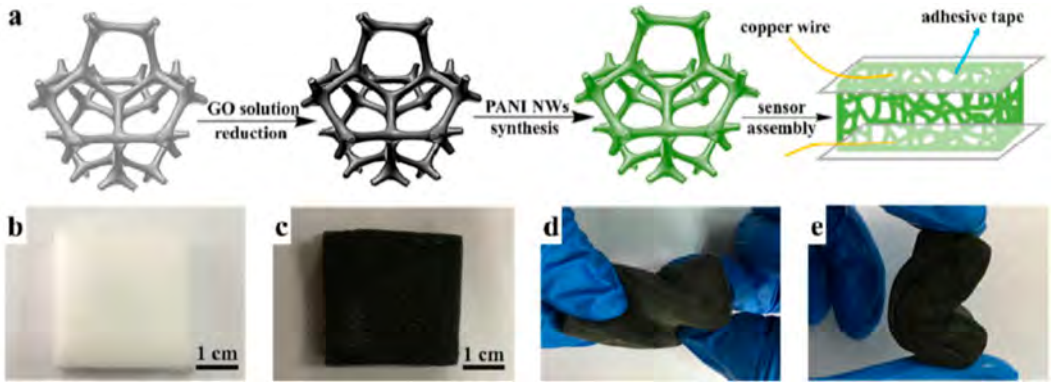

Figure 10. (a) Fabrication process of the flexible pressure sensor. (b, c) Photographs of pristine sponge and rGO/polyaniline wrapped sponge (RGPS). (d, e) Photographs of the twisted and folded RGPS. Reprinted with permission from ref 94. Copyright 2018 Royal Society of Chemistry.

enables the sponge being not only conductive but also hydrophobic, therefore the WS_2 coated sponge can be used in wet/sweat and underwater conditions.[146]

In Situ Polymerization Coating of a Template Sponge. To fulfill better adhesion, conducting polymer can be in situ polymerized on the polymer sponge.[147] Brady et al.[86] and Luo et al.[93] prepared conductive sponge by coating a layer of PPy on PU or cellulose sponge respectively via chemical oxidative polymerization. Ge et al.[94] fabricated a synergetic rGO/PANI wrapped sponge (RGPS) by a two-step method. As shown in Figure 10, a layer of graphene was first wrapped on the MF sponge by dip coating and reduction; another layer of PANI was then coated on the rGO/MF sponge by in situ polymerization. In this sponge, the graphene was negatively charged, while PANI was positively charged; therefore, they had good adhesion and stability.

Wet-Chemical Deposition on a Template Sponge. Figure 11 shows a typical process of "polymer-assisted electroless metal deposition" method, which combines ion exchange and electroless metal deposition processes to coat a metal layer on a sponge.[73,87,148] PDMS sponge was treated with air plasma and coated with a layer of vinyltrimethoxysilane (VTMS) via silanization; the resultant VTMS-PDMS sponge was covalently attached to poly(2-(methacryloyloxy)-ethyl-trimethylammonium chloride) (PMETAC) by radical polymerization; finally, the PMETAC-modified PDMS sponge was coated with a metal (e.g., Cu, Ag/Cu, Au/Cu) layer by electroless metal deposition.[73]

Layer-by-Layer Assembly on a Template Sponge. Carbon materials (e.g., CB, CNTs, and graphene) usually have poor dispersibility and are easily aggregated in solvent, which makes them difficult to form uniform dispersion. To improve their dispersibility, these materials can be modified/stabilized by charged polymer/surfactant. For example, CB can be negatively charged by adding cellulose nanocrystal (CNC), and be positively charged by adding chitosan (CS). Wu et al.[58] developed a layer-by-layer assembly method to coat CB with different surface charges on a polymer sponge; as shown in Figure 12, the sponge was dipped inthe positively charged CB^+ and negatively charged CB^- dispersion alternatively. The oppositely charged and well suspended CB made it feasible to form controllable conductive layers on the sponge with strong adhesion. Ma et al.[36] prepared MWCNT/RGO@PU sponge using similar method by alternatively dipping the PU sponge between positively charged $MWCNT^+$ and negatively charged GO^-.

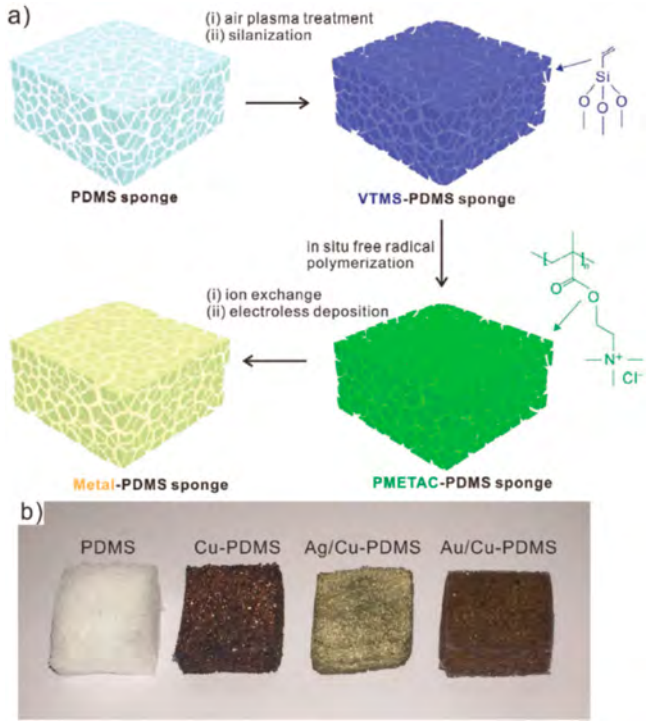

Figure 11. (a) Schematic illustration of the fabrication of metal-coated PDMS sponges. (b) Optical images of the original PDMS sponge and the as-prepared Cu-, Ag/Cu-, and Au/Cu-PDMS sponge. The resistance of the as-made Cu-, Ag/Cu-, and Au/Cu-PDMS sponge was 1.79, 2.10, and 0.86 Ω cm^{-1}, respectively. Reprinted with permission from ref 73. Copyright 2016 John Wiley and Sons.

4. PERFORMANCE AND APPLICATION EXAMPLES

4.1. General Features of Pressure Sensor Assembled from 3D Conductive Sponge. The piezoresistive pressure sensor is a resistive-type sensor; the recognized output signal of the device is the electrical resistance, which varies in response to the deformation (e.g., compression, torsion, bend) of the device. To evaluate the performance of a pressure sensor, several key parameters including applied strain (or pressure), resistance change ($\Delta R/R_0$), and sensitivity or gauge factor (GF) are assessed. As shown in Figure 13, when a pressure (ΔP) is applied on a sponge, the compression strain (ε) is expressed as $\varepsilon = \Delta L/L_0 = (L_0 - L)/L_0 \times 100\%$, where L_0 is the initial length of the sponge, and L is the length of the sponge under compression; the resistance change ($\Delta R/R_0$) is expressed as $\Delta R/R_0 = (R - R_0)/R_0 \times 100\%$, where R_0 is the initial resistance of the conductive sponge, and R is the resistance of the sponge under compression; the sensitivity (e.g., GF) of a pressure sensor is defined as GF = $(\Delta R/R_0)/\varepsilon$, which evaluates the sensitivity of the device to the strain, or GF = $(\Delta R/R_0)/\Delta P$, which evaluates the sensitivity of the device to the change of the applied pressure.

DOI: 10.1021/acsami.8b20929
ACS Appl. Mater. Interfaces 2019, 11, 6685−6704

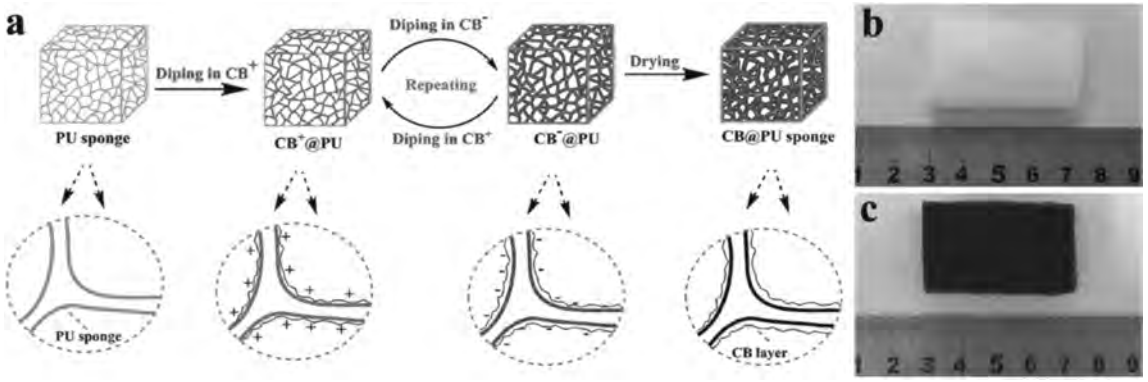

Figure 12. (a) Schematic diagram for preparation of CB@PU sponges. (b) Photographs of a neat PU sponge and (c) CB@PU sponge. Reprinted with permission from ref 58. Copyright 2016 John Wiley and Sons.

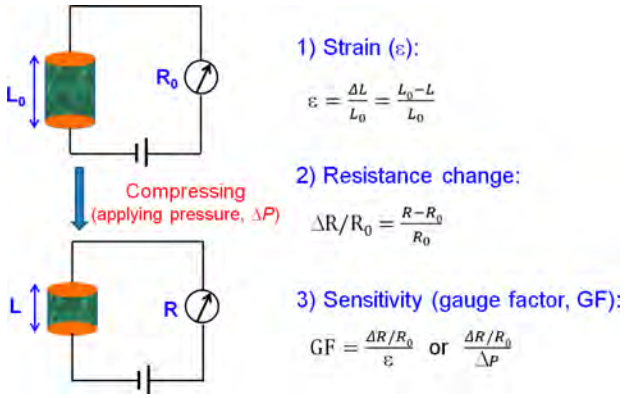

Figure 13. Schematic showing the working principle of a pressure sensor based on 3D conductive sponge, and the key parameters for evaluating the performance of pressure sensor.

Highly compressible conductive sponge is a promising material for piezoresistive pressure sensor application. A pressure sensor can be simply assembled from a 3D conductive sponge by adding electrodes at the two ends/sides of the sponge. Most reported 3D conductive sponges are highly compressible; some can be compressed to more than 80% strain or to the pressure range from 0 to about tens or hundreds of kilopascal (kPa). In general, the pressure related to the normal human activity is distributed in the range of 1 Pa ∼ 100 kPa, which can be categorized into three pressure regimes: (1) subtle-pressure regime from 1 Pa to 1 kPa (e.g., human skin sensing), (2) low-pressure regime from 1 to 10 kPa (e.g., gentle manipulation of objects), and (3) medium-pressure regime from 10 to 100 kPa (e.g., blood pulse, human weight, and joint movements).[17] Therefore, the piezoresistive pressure sensor made from 3D conductive sponge is sufficient to detect most human motions. Table 1 summarizes the performance parameters (including strain/pressure, resistance change and/or sensitivity, and stability) of the pressure sensors fabricated from different types of conductive sponges.

Other important parameters that need to be assessed/evaluated include response time, limit of detection, linearity, reproducibility/stability, and hysteresis effect.[17,23,24] These parameters are strongly correlated to the material/structure of the conductive sponge and the practical application condition such as the intrinsic plastic behavior of the sponge material, the pore size/structure of the sponge, the density of the sponge, and the compression frequency. Other properties of the material may also need to be considered in the development of wearable pressure sensor; for example, biocompatibility of the material is important for wearable application.

The piezoresistive pressure sensor made from 3D conductive sponge typically has negative piezoresistive effect, i.e., the resistance of the sensor decreases upon compression. The negative piezoresistive effect can be attributed to the fact that when compressed, more contact areas/points are formed between the skeletons of the sponge, resulting in more conductive pathways and thus decrease of the electric resistance. Figure 14 shows a schematic illustration of the conductive network and an equivalent circuit diagram to simulate the electric resistance change of a graphene coated sponge.[91] In the graphene coated sponge, the polymer skeleton wrapped with graphene was considered as a resistor network. The network structure was not evenly deformed during the process of compression. At small strain, the cells of the outer layers were flattened first, and the corresponding conductive connections were formed at the outer layers, leading to large decrease of resistance; with increased strain, the cells of the middle layers were compressed to an oval shape with increased deformation, but no new conductive connection was formed, resulting in small decrease in resistance; at large strain, all cells became flattened and a large number of conductive connections were formed, leading to a continuous decrease of resistance.[91] Therefore, the pressure sensor based on 3D conductive sponge typically has different sensitivity at different applied strain or pressure range.

Depending on the material/structure of a conductive sponge, other sensing mechanisms are possible. For the sensor of 3D conductive sponge prepared by coating carbon black or metal (e.g., Au) nanoparticles on polymer sponge,[58,59] the resistance may increase at small applied strain but decrease at high strain. Wu et al. reported an example of such change.[58] When a pressure was applied upon the CB@PU sponge (Figure 15a), microcrack junctions in the CB layer were disconnected; the breakage of the local conductive pathways resulted in increase of the electric resistance (or decrease of the current), as shown in the yellow area in Figure 15b-c. As the compressive strain gradually increased, the crack-gap and crack-density extended correspondingly, which further decreased the conductivity of the CB layers (Figure 15a middle). When the applied strain reached a certain value, at which the CB@PU backbones started to be in contact, more conductive pathways were formed between the CB layer (Figure 15a

DOI: 10.1021/acsami.8b20929
ACS Appl. Mater. Interfaces 2019, 11, 6685−6704

Table 1. Summary of the Performance of Recently Reported Piezoresistive Pressure Sensors Based on 3D Conductive Sponges

			device performance					
	material	preparation method	device size	compressive strain or pressure range	sensitivity ($\Delta R/R_0$ or GF)	stability (cycle tested)	application	ref
neat conductive sponge	CNTs foam	chemical vapor deposition (CVD)	N/A	0–95%	$\Delta R/R_0 = -13\%$	1000 cycles	N/A	54
	graphene foam	freeze-drying	1 cm × 1 cm ×1 cm	0–60%	GF = −1.3	N/A	N/A	75
	graphene block	(1) egg beater sparking; (2) freeze-drying	2 mm × 7 mm × 7 mm	0–95% (i.e., 0–2 kPa)	229.8 kPa^{-1} (0–0.1 kPa) 26.86 kPa^{-1} (0.4–1 kPa)	100 000 cycles	gentle pressure sensing	38
	rGO foam	freeze-drying	diameter4.5 cm thickness 2 mm	0.1–200 Pa	22.8 kPa^{-1} (0–10 Pa) 1.34 kPa^{-1} (>10 Pa)	5000 cycles	human motion detection (finger bending)	40
	graphene aerogel	(1) dip-coating; (2) template removal by dissolving	N/A	0–95% (0.556 MPa)	0.18 kPa^{-1}	100 cycles	human motion detection (finger bending)	138
	graphene/CNTs aerogel	(1) hydrothermal (2) freeze-drying	5 mm × 4 mm × 3 mm	0–90%	GF = −2.3 @30% GF = −1.25@60%	100 cycles	light switch	105
	graphene/amorphous carbon hierarchical foam	(1) chemical vapor deposition (CVD) (2) etching	thickness 2 mm	0–50%	$\Delta R/R_0 = -39\%$ (GF = −7.9) @5% strain	200 cycles	N/A	134
	MXene/rGO aerogel	freeze-drying	N/A	0–3.5 kPa	4.05 kPa^{-1} (0–1 kPa) 22.56 kPa^{-1} (>1 kPa)	10 000 cycles	light switch; human motion detection (speaking, venous pulse, arterial pulse)	106
	Cu nanowire aerogel	freeze-drying	N/A	0–60% (0–200 Pa)	0.02–0.7 kPa^{-1}	200 cycles	N/A	56
	PPy sponge	supercritical fluid drying	N/A	0–90% strain	$\Delta R/R_0 = -3\%$	N/A	N/A	57
	Zn_2GeO_4@PPy nanowire aerogel	freeze-drying	length 1 cm, cross-sectional area 0.25 cm^2	0–90% strain	0.38 kPa^{-1} (0–1.5 kPa); 0.076 kPa^{-1} (>1.5 kPa)	1000 cycles	light switch, pressure sensor array (3 × 3)	61
	natural-wood-derived carbon sponge	(1) chemical treating and freeze-drying (2) carbonization (1000 °C)	10 mm × 5 mm × 1 mm	0–80% (0–70 kPa)	N/A	10 000 cycles	light switch human motion detection (finger bending)	63
	melamine-sponge-derived carbon	carbonization (800 °C)	1 cm ×1 cm	0–10 kPa	100.29 kPa^{-1} (0–2kPa); 21.22 kPa^{-1} (>2 kPa)	11 000 cycles	human motion detection (breathing, arterial pulse, finger bending)	76
	melamine-sponge-derived carbon/CNTs	(1) carbonization (1000 °C) (2) soaking in CNT ink	1 cm × 1 cm ×1 cm	0–80%	GF = −800% (80%)	240 000 cycles	human motion detection (finger bending)	126
composite conductive sponge	graphene/PU composite sponge	(1) mix and freeze (2) freeze-drying	N/A	0–90% strain	GF = 2.45 (0–60%); GF = 12.24 (60–90%)	10 cycles	N/A	34
	graphene/polyimide	(1) mix and freeze (2) freeze-drying (3) annealing	N/A	0–6.5 kPa	0.18 kPa^{-1} (0–1.5 kPa); 0.023 kPa^{-1} (3.5–6.5 kPa)	2000 cycles	N/A	112
	CNTs/PU	(1) mixing	Diameter 15 mm; thickness 10 mm	0–85.6%	GF = 1.22 (0–77%); GF = 0.06 (77–85.6%)	2000 cycles	human motion detection (joint bending, and walking)	67

ACS Appl. Mater. Interfaces 2019, 11, 6685–6704
DOI: 10.1021/acsami.8b20929

Table 1. continued

			device performance					
	material	preparation method	device size	compressive strain or pressure range	sensitivity ($\Delta R/R_0$ or GF)	stability (cycle tested)	application	ref
		(2) directional freeze-drying		(0−11.27 MPa)				
	CNT/PU/epoxy composite sponge	(1) mix and freeze		0−70%	$\Delta R/R_0 \approx$ 0.4−1.0	2000 cycles	light switch; walking	64
		(2) freeze-drying						
		(3) annealing						
	CNT/polyimide sponge	(1) preparation of PAA	diameter 11 mm; height 10 mm	0−80%	$\Delta R/R_0 \approx$ 0−1.0 (R decrease obvious at <15% strain)	10 cycles	N/A	66
		(2) mixing and freeze-drying						
		(3) thermal imidization						
	3D CNF/PAN/PI nanofibrous sponge	(1) preparation of PAN, PI, and carbon nanofibers	diameter 10 mm; height 20 mm	0−80%	GF ≈ −1 to 9	2000 cycles	light switch, pressure sensor array (5 × 5)	65
		(2) mixing and freeze-drying						
		(3) thermal annealing						
	carbonaceous nanofibrous aerogel	(1) mixing, freezing, and freeze-drying	10 mm × 10 mm × 2 mm	0−60%	0.43 kPa^{-1} (0−3 kPa); 1.02 kPa^{-1} (>3 kPa)	100 cycles	monitoring neck pulse	122
		(2) carbonization						
conductive sponge impregnated with elastomer	graphene porous network/PDMS	(1) graphene growth on Ni foam by CVD	N/A	0−2000 kPa	GF = 2.6 (0−18%)	10 cycles	human motion detection (finger bending, blood pressure)	70
		(2) PDMS infiltration			GF = 8.5 (22−40%)			
		(3) Ni etching						
	gollow structured graphene/PDMS	(1) graphene growth on Ni foam by CVD	3 mm ×3 mm	0−60 kPa	15.9 kPa^{-1} (0−60 kPa)	26 000 cycles	wrist blood pressure monitoring, tactile sensing unit for robot hand operation	81
		(2) PDMS infiltration						
		(3) Ni etching						
	graphene/silane	(1) freeze-drying	N/A	99.50%	67.1 kPa^{-1} (30−500 Pa); 8.6 kPa^{-1} (0.8−1.5kPa); 14.3 kPa^{-1} (>1.5 kPa)	10 cycles	N/A	109
		(2) vapor polymerization of silane		0−2.5 kPa				
	graphene/Polyimide	(1) hydrothermal freezing	diameter 10 mm; height 10 mm	0−90%	$\Delta R/R_0$ = −68% @90% strain	300 cycles	N/A	82
		(2) infiltrating						
		(3) curing						
	PPy@Graphene/PDMS	(1) electrochemical polymerization of PPy	N/A	0−50%	N/A	500 cycles	human motion detection (elbow bending)	68
		(2) Ni etching						
		(3) PDMS infiltration						
	melamine-sponge-derived carbon sponge/silicone	(1) carbonization (1000 °C)	thickness 2.4 mm	0−40% strain	GF = −4.3 (0−10%)	1000 cycles	human motion detection (wrist bending, eye blinking, blood pulse, and breathing)	66

ACS Appl. Mater. Interfaces 2019, 11, 6685−6704 DOI: 10.1021/acsami.8b20929

Table 1. continued

	material	preparation method	device performance: device size	compressive strain or pressure range	sensitivity ($\Delta R/R_0$ or GF)	stability (cycle tested)	application	ref
		(2) encapsulation of silicone resin			GF = −18.4 (10−25%)			
					GF = −8.4 (25−40%)			
	MOF-derived carbon/PDMS	(1) carbonization (800 °C)	N/A	0−2000 Pa	15.63 kPa^{-1}	2000 cycles	human motion detection (wrist pulse)	69
		(2) encapsulation of PDMS						
conductive-material-coated sponge	graphene@PU sponge	dip coating and hydrothermal reduction	2 mm × 2 mm × 0.2 mm	0−10 kPa	0.26 kPa^{-1} (0−2 kPa); 0.03 kPa^{-1} (2−10 kPa)	10 000 cycles	pressure sensor array (11 × 13)	74
	graphene@PU sponge	immersing and drying	1.5 cm × 1.5 cm × 1.5 cm	0−640 kPa	1.04 kPa^{-1} (13−260 Pa); 0.12 kPa^{-1} (260 Pa ∼ 20 kPa)	N/A	detection of surface roughness for tactile sensing	88
	graphene@PU sponge	(1) dip coating and hydrothermal reduction	diameter 10 mm; height 12 mm	0−99%	0.75−3.08 kPa^{-1}	N/A	N/A	72
		(2) freeze-drying						
	CNTs@PDMS sponge	(1) preparation of PDMS sponge	N/A	0−60%	GF = 5.6 (0.3 kPa^{-1}) @<2.5% (<1 kPa)	255 cycles	N/A	90
		(2) drop casting		0−50 kPa	GF = 1.16 (0.9 kPa^{-1}) @2.5−60% (15−501 kPa)			
	rGO@PU or PVC sponge	(1) preparation of graphene oxide solution	N/A	0−70% strain	maximum sensitivity: 0.91 N^{1-}& 1.03 N^{1-}	80 cycles	human motion detection (finger bending)	91
		(2) dip coating						
		(3) reduced by heating						
	Carbon black@PU sponge	layer-by-layer assembly (alternatively coating)	4 mm ×4 mm	0−60%	0.068 kPa^{-1} (0−9%); 0.023 kPa^{-1} (9−52%); 0.036 kPa^{-1} (52−60%)	50 000 cycles	human motion monitoring (speaking, coughing, swallowing, pulse, breathing, and joint bending)	58
	CNT/rGO@PU sponge	layer-by-layer assembly (alternatively coating)	N/A	0−75%	GF = −0.96to 1.75	N/A	human motion monitoring (finger and elbowt bending)	36
				(i.e., 0−5.6 kPa)				
	CNT/rGO@PU sponge	dip coating	13 mm × 8 mm × 5 mm	0−100%	0.022 kPa^{-1} (0−2.7 kPa)	5000 cycles	human motion detection (finger bending)	60
				(i.e., 0−48.8 kPa)	0.088 kPa^{-1} (2.7−10 kPa)			
					0.034 kPa^{-1} (>10 kPa)			
	Au@PU sponge	sputtering	10 mm × 10 mm × 10 mm	0−60%	GF = 1.09 (0−23%); GF = 1.37 (23−47%);GF = 4.43 (47−60%)	1000 cycles	speech recognition, heart beating, sound waves, vehicle speed detection	59
	PEDOT:PSS@melamine sponge	dip coating	diameter 10 mm; height 10 mm	0−80%	$\Delta R/R_0$ = 0 to −90%	1000 cycles	human motion monitoring (speaking, joint bending, and walking), and prototype of sensory array (3 × 3)	19
					GF = −1.10 to −2.30			
	rGO/PANi@melamine sponge	(1) immersing in GO solution and reduction	2 cm × 1 cm × 0.5 cm	0−27 kPa	0.152 kPa^{-1} (0−3.24 kPa)	9000 cycles	human motion monitoring (voice recognition, swallowing, mouth opening, blowing, breathing, and joint bending)	94
		(2) polymerization of PANi			0.0049 kPa^{-1} (13.32−27.39 kPa)			
					0.034 kPa^{-1} (>10 kPa)			

ACS Appl. Mater. Interfaces 2019, 11, 6685−6704 DOI: 10.1021/acsami.8b20929

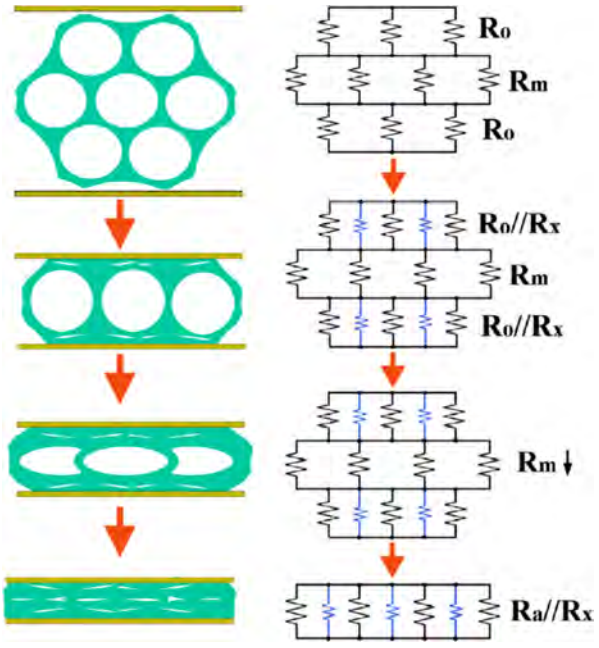

Figure 14. Schematic illustrations of network structure change of 3D conductive sponge and its equivalent circuit diagram in explanation of the working mechanism of pressure sensor. Reprinted with permission from ref 91. Copyright 2017 Elsevier.

right), leading to decrease of the electrical resistance (blue and pink regions of Figure 15b, c). These two mechanisms worked simultaneously; and the synergistic effect on the pressure-sensing behavior enabled the CB@PU sponge not only to detect deformations over wide range of strain/pressure but also to detect small strain/pressure with a high sensitivity.[58]

4.2. Human Motion Detection/Monitoring Application. As mentioned above, the detection range of a pressure sensor based on 3D conductive sponge can fulfill the requirement of monitoring the pressure change during most human activities. Generally, a pressure sensor is attached on human body or mounted on wearable textile/cloth to detect the human motion. To detect a subtle motion such as wrist pressure, speaking, and breathing, the sensor is built up as a skin-conformable device that can be tightly attached on the skin at the position of wrist or neck. Because the signals of these subtle motions are very small, the conformable and tight attachment is key to improving the sensitivity and avoiding noise. For example, as shown in Figure 16a, a poly(3,4-ethylenedioxythiophene):poly- (styrenesulfonate)@melamine sponge (PEDOT:PSS@MS) pressure sensor was mounted on the human neck, which could detect human speaking.[19] The signals of different words were significantly different, which was attributed to the different muscle movements when pronouncing the words. Results demonstrated that the pressure sensor could be used in a speech recognition system. To detect vigorous motions such as joint bending, walking, and body movements, pressure sensors were attached to the joint positions, in which their movement could lead to the deformation of the sponges. As shown in Figure 16b–d, a pressure sensor attached at the finger, elbow, and knee could detect bending of the finger, elbow and knee, respectively. In addition, by mounting three devices in an insole (as shown in Figure 16e-g), the devices could monitor the human walking gait.[19] Therefore, these pressure sensors were capable of providing real-time information on human body conditions for various activities such as athlete training and patient physical therapy. Such pressure sensors could also have potential applications in human—machine interaction, robotic arms, etc.

4.3. Electronic Skin Application. Another important application of pressure sensor is electronic skin (e-skin). The human skin is the largest organ of human body that can sense force, temperature, and other stimuli. Mimicry of the human skin is of great research interests in robotics, artificial

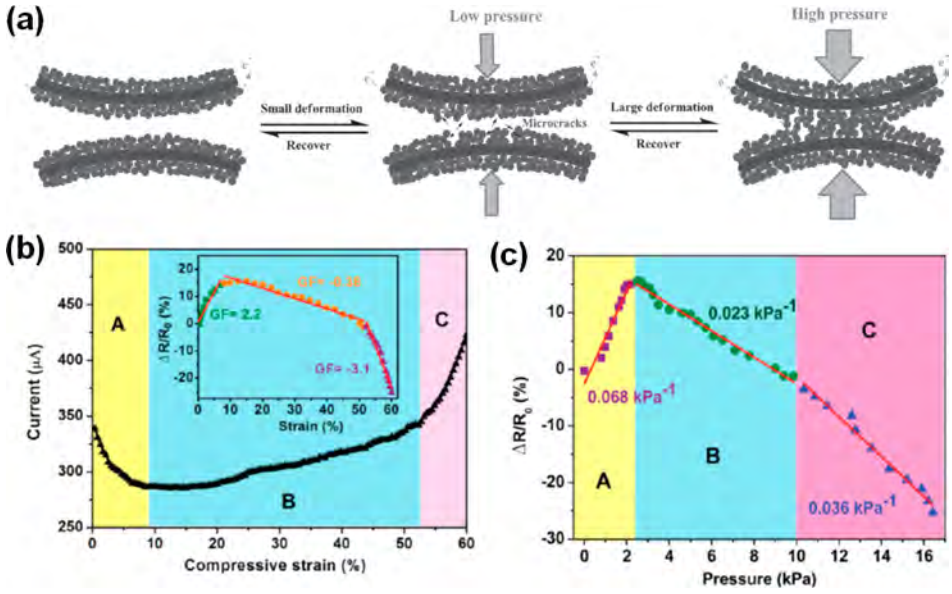

Figure 15. (a) Schematic evolutions of the conductive pathways in a CB@PU sponge during continuous compressive deformation. Disconnection of microcrack junctions in the CB layer occurred upon small deformations and caused breakage of local conductive pathways (middle). CB@PU backbones contacted with each other upon large deformations, leading to formation of more conductive pathways in the CB layer (right). (b) Responsive current curve of a CB@PU sponge versus compressive strain along with the corresponding GF variation (inset). (c) Relative resistance change ($\Delta R/R_0$) versus progressively increasing pressure. Reprinted with permission from ref 58. Copyright 2016 John Wiley and Sons.

DOI: 10.1021/acsami.8b20929
ACS Appl. Mater. Interfaces 2019, 11, 6685–6704

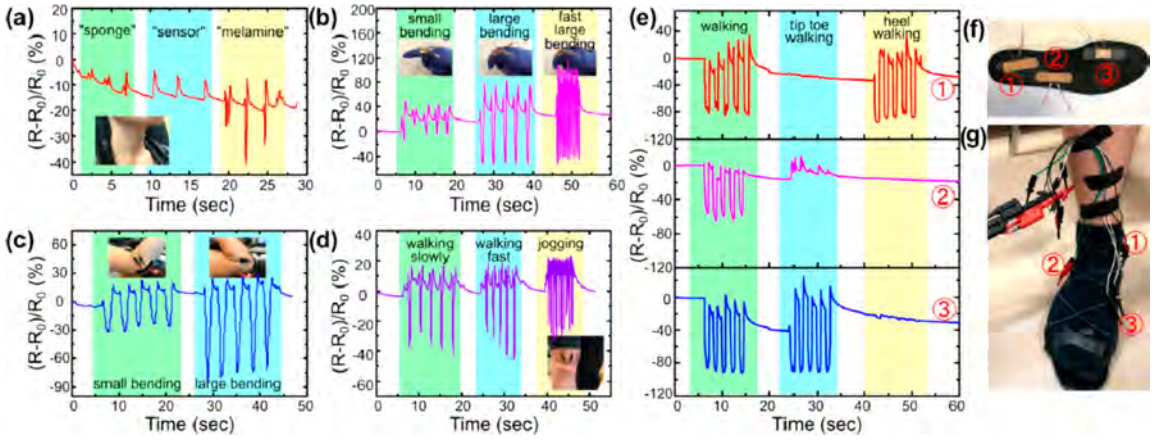

Figure 16. (a) Applications of the PEDOT:PSS@MS pressure sensor for human motion detection: (a) relative resistance variations of the sensor attached on the throat induced by phonation of sponge, sensor, and melamine; (b) relative resistance variations of the sensor attached on the index finger induced by bending; (c) relative resistance variations of the sensor attached on the elbow induced by bending; (d) relative resistance variations of the sensor attached on the knee joint induced by walking; (e) relative resistance variations of the sensors attached to an insole induced by walking; (f—g) photographs showing the three sensors attached to the insole and dressed on foot for testing. Reprinted with permission from ref 19. Copyright 2018 American Chemical Society.

intelligence, and biomedical applications.[16] Array of pressure sensors plays a key role in mapping and sensing force/pressure, which is an important function in e-skin. Xu and Ding et al. reported prototype of a pressure sensor array based on conductive sponge.[65] As shown in Figure 17, a sensor array of 5 pixel ×5 pixel sensor units was fabricated using small cylindrical conductive sponge. The sensor array could map out the force distribution of an AA battery placed on top of it.[65]

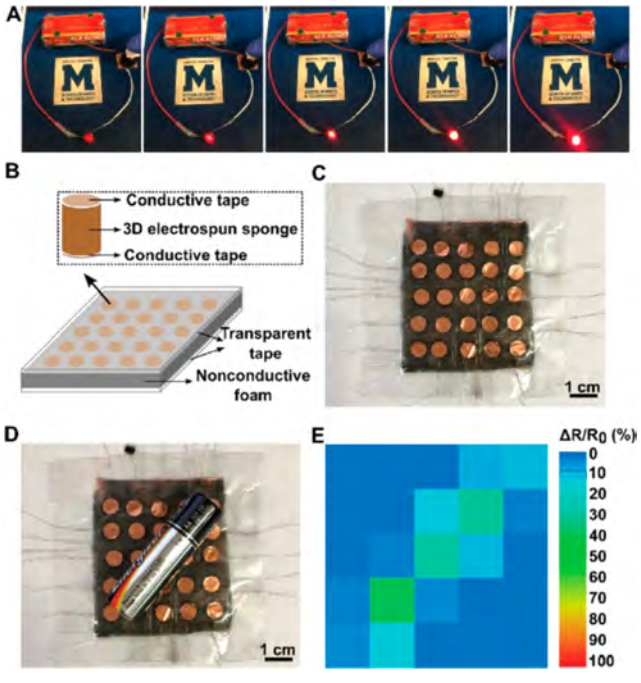

Figure 17. (A) LED circuit with the 3D conductive sponge as a compressible switch. (B) Schematic of a proof-of-concept matrix of sensor array, containing 5 pixel ×5 pixel pressure sensor units. (C) Photograph of the sensor array. (D) Photograph of the sensor array with a battery placed on top. (E) 2D mapping of the resistance changes corresponding to the pressure applied by the battery on the sensor array. Reprinted with permission from ref 65. Copyright 2017 Royal Society of Chemistry.

Such a proof-of-concept electronic skin still has a long way toward practical application. Advanced engineering design is needed to further develop e-skin based on the sponge-based pressure sensor. Furthermore, integration with other sensors to design multifunctional sensory systems, as well as improving the sensitivity and accuracy, is critical for development of e-skin.

5. CONCLUDING REMARKS AND PERSPECTIVE

In the past few years, tremendous progress has been made on flexible and wearable sensors by development of various novel materials/structures. In this review, we summarize the recent advances in flexible and wearable piezoresistive pressure sensors based on 3D monolithic conductive sponges. The newly emerging materials and methods used in fabrication of the 3D conductive sponge are comprehensively illustrated. In addition, device performance and applications of these sponge-based pressure sensors in human motion detection/monitoring and e-skin are highlighted. Successful outcomes from these efforts shine a bright light on the potential applications of the pressure sensor based on conductive sponge in next-generation wearable sensor products for real-time human health monitoring, as well as modern soft robotics and artificial intelligence systems.

To implement these high-performance sponge-based pressure sensors for practical applications, several imminent challenges need to be further investigated. (1) For the materials/devices, device standardization and modeling/simulation are needed to understand the correlation between the performance of the pressure sensor and the structures (e.g., pore size/size distribution, dimensions, etc.) of the 3D conductive sponges, which may help design of spongy materials with good linearity and sensitivity over wide ranges of pressure/strain.[149] (2) For "truly" flexible pressure/strain sensor circuitry, integration of the sensors with flexible and reliable electric contacts and connectors, as well as design of systems that meet the specific wearable requirement (e.g., conformability with the body parts), would require innovative patterning and processing techniques.[150] (3) For applications in real-time human health monitoring, as well as modern soft robotics and artificial intelligence systems, significant multi-

DOI: 10.1021/acsami.8b20929
ACS Appl. Mater. Interfaces 2019, 11, 6685−6704

disciplinary efforts are needed to develop wearable sensory systems that integrate multifunctional sensors (e.g., temperature, pressure, physiology signals etc.), power system (e.g., battery), and real-time data transmission module.[151] Wireless and/or self-powered sensors are reported recently to address the power supply and data transmission issues.[152,153] (4) Last, but not the least, the stability and biocompatibility of the conductive sponges and the devices based on these materials are important for wearable applications, which needs to be addressed. The long-term stability of the materials/devices at the real working conditions (e.g., daily use under various human sweating and body temperature conditions) is largely unexplored. Work in these areas would be important steps in moving flexible and wearable pressure sensors based on piezoresistive 3D monolithic conductive sponges toward future practical applications.

AUTHOR INFORMATION

Corresponding Author

*Email: Zhengtao.Zhu@sdsmt.edu.

ORCID

Yichun Ding: 0000-0002-7441-800X

Hao Fong: 0000-0002-1497-5162

Zhengtao Zhu: 0000-0002-9311-2110

Author Contributions

The manuscript was written through contributions of all authors. All authors have given approval to the final version of the manuscript.

Notes

The authors declare no competing financial interest.

ACKNOWLEDGMENTS

This work is supported by the National Aeronautics and Space Administration (NASA Cooperative Agreement 80NSSC18M0022) and Program of Biomedical Engineering at South Dakota School of Mines & Technology.

ABBREVIATIONS

Bubble-derived graphene foam, BGF; Carbon black, CB; Carbon nanofiber, CNF; Carbon nanotube, CNT; Carbonaceous nanofibrous aerogel, CNFA; Cellulose nanocrystal, CNC; Chemical vapor deposition, CVD; Chitosan, CS; Electronic skin, e-skin; Gauge factor, GF; Graphene oxide, GO; KGM/SiO_2 nanofiber composite aerogel, KNFA; Konjac glucomannan, KGM; Melamine-formaldehyde, MF; Melamine sponge, MS; Metal−organic framework, MOF; Microelectromechanical systems, MEMS; Microporous PDMS, pPDMS; Wood carbon sponge, WCS; Multiwalled carbon nanotube, MWCNT; Partially reduced GO, pr-GO; Physical vapor deposition, PVD; Poly(3, 4-ethylenedioxythiophene):poly(styrenesulfonate), PEDOT:PSS; Polyacrylonitrile, PAN; Polyaniline, PANI; Polydimethylsiloxane, PDMS; Polyimide, PI; Polypyrrole, PPy; Polyurethane, PU; Polyvinylidene fluoride, PVDF; Reduced graphene oxide, rGO; rGO/polyaniline wrapped sponge, RGPS; Sparkling graphene block, SGB; Thermoplastic polyurethane, TPU; Three-dimensional, 3D; Vinyltrimethoxysilane, VTMS; 2-(methacryloyloxy)ethyl-trimethylammonium chloride, PMETAC

REFERENCES

(1) Bao, Z.; Chen, X. Flexible and Stretchable Devices. *Adv. Mater.* **2016**, *28*, 4177−4179.

(2) Gao, W.; Emaminejad, S.; Nyein, H. Y. Y.; Challa, S.; Chen, K.; Peck, A.; Fahad, H. M.; Ota, H.; Shiraki, H.; Kiriya, D.; Lien, D.-H.; Brooks, G. A.; Davis, R. W.; Javey, A. Fully Integrated Wearable Sensor Arrays for Multiplexed in Situ Perspiration Analysis. *Nature* **2016**, *529*, 509.

(3) Patel, S.; Park, H.; Bonato, P.; Chan, L.; Rodgers, M. A Review of Wearable Sensors and Systems with Application in Rehabilitation. *Journal of NeuroEngineering and Rehabilitation* **2012**, *9*, 21.

(4) Yang, Y.; Gao, W. Wearable and Flexible Electronics for Continuous Molecular Monitoring. *Chem. Soc. Rev.* **2018**, *1*, 580.

(5) Haghi, M.; Thurow, K.; Stoll, R. Wearable Devices in Medical Internet of Things: Scientific Research and Commercially Available Devices. *Healthc Inform Res.* **2017**, *23*, 4−15.

(6) Jin, H.; Shibli, A. R. Y.; Hossam, H. Advanced Materials for Health Monitoring with Skin Based Wearable Devices. *Adv. Healthcare Mater.* **2017**, *6*, 1700024.

(7) Cardinale, M.; Varley, M. C. Wearable Training-Monitoring Technology: Applications, Challenges, and Opportunities. *International Journal of Sports Physiology and Performance* **2017**, *12*, S2-55−S52-62.

(8) Bandodkar, A. J.; Jeerapan, I.; Wang, J. Wearable Chemical Sensors: Present Challenges and Future Prospects. *ACS Sensors* **2016**, *1*, 464−482.

(9) Heikenfeld, J.; Jajack, A.; Rogers, J.; Gutruf, P.; Tian, L.; Pan, T.; Li, R.; Khine, M.; Kim, J.; Wang, J.; Kim, J. Wearable Sensors: Modalities, Challenges, and Prospects. *Lab Chip* **2018**, *18*, 217−248.

(10) Ding, Y.; Yang, J.; Tolle, C. R.; Zhu, Z. A Highly Stretchable Strain Sensor Based on Electrospun Carbon Nanofibers for Human Motion Monitoring. *RSC Adv.* **2016**, *6*, 79114−79120.

(11) Kenry; Yeo, J. C.; Lim, C. T. Emerging Flexible and Wearable Physical Sensing Platforms for Healthcare and Biomedical Applications. *Microsystems & Nanoengineering* **2016**, *2*, 16043.

(12) Wang, H.; Xiaohua, M.; Yue, H. Electronic Devices for Human Machine Interfaces. *Adv. Mater. Interfaces* **2017**, *4*, 1600709.

(13) Wang, J.; Lin, M.-F.; Park, S.; Lee, P. S. Deformable Conductors for Human−Machine Interface. *Mater. Today* **2018**, *21*, 508.

(14) Rich, S. I.; Wood, R. J.; Majidi, C. Untethered Soft Robotics. *Nature Electronics* **2018**, *1*, 102−112.

(15) Jason, N. N.; Ho, M. D.; Cheng, W. Resistive Electronic Skin. *J. Mater. Chem. C* **2017**, *5*, 5845−5866.

(16) Wang, X.; Dong, L.; Zhang, H.; Yu, R.; Pan, C.; Wang, Z. L. Recent Progress in Electronic Skin. *Advanced Science* **2015**, *2*, 1500169.

(17) Zang, Y.; Zhang, F.; Di, C.-a.; Zhu, D. Advances of Flexible Pressure Sensors toward Artificial Intelligence and Health Care Applications. *Mater. Horiz.* **2015**, *2*, 140−156.

(18) Ge, G.; Wei, H.; Jinjun, S.; Xiaochen, D. Recent Progress of Flexible and Wearable Strain Sensors for Human-Motion Monitoring. *J. Semicond.* **2018**, *39*, 011012.

(19) Ding, Y.; Yang, J.; Tolle, C. R.; Zhu, Z. Flexible and Compressible PEDOT:PSS@Melamine Conductive Sponge Prepared Via One-Step Dip Coating as Piezoresistive Pressure Sensor for Human Motion Detection. *ACS Appl. Mater. Interfaces* **2018**, *10*, 16077−16086.

(20) Yang, T.; Xie, D.; Li, Z.; Zhu, H. Recent Advances in Wearable Tactile Sensors: Materials, Sensing Mechanisms, and Device Performance. *Mater. Sci. Eng., R* **2017**, *115*, 1−37.

(21) Trung, T. Q.; Nae Eung, L. Flexible and Stretchable Physical Sensor Integrated Platforms for Wearable Human Activity Monitoringand Personal Healthcare. *Adv. Mater.* **2016**, *28*, 4338−4372.

(22) Wang, F.; Liu, S.; Shu, L.; Tao, X.-M. Low-Dimensional Carbon Based Sensors and Sensing Network for Wearable Health and Environmental Monitoring. *Carbon* **2017**, *121*, 353−367.

(23) Zhao, S.; Li, J.; Cao, D.; Zhang, G.; Li, J.; Li, K.; Yang, Y.; Wang, W.; Jin, Y.; Sun, R.; Wong, C.-P. Recent Advancements in Flexible and Stretchable Electrodes for Electromechanical Sensors: Strategies, Materials, and Features. *ACS Appl. Mater. Interfaces* **2017**, *9*, 12147−12164.

DOI: 10.1021/acsami.8b20929
ACS Appl. Mater. Interfaces 2019, 11, 6685−6704

(24) Amjadi, M.; Kyung, K. U.; Park, I.; Sitti, M. Stretchable, Skin Mountable, and Wearable Strain Sensors and Their Potential Applications: A Review. *Adv. Funct. Mater.* **2016**, *26*, 1678−1698.
(25) Chen, S.; Kai, J.; Zheng, L.; Di, C.; Guozhen, S. Recent Developments in Graphene Based Tactile Sensors and E Skins. *Advanced Materials Technologies* **2018**, *3*, 1700248.
(26) Fan, F. R.; Wei, T.; Lin, W. Z. Flexible Nanogenerators for Energy Harvesting and Self Powered Electronics. *Adv. Mater.* **2016**, *28*, 4283−4305.
(27) Zhang, R.; Hu, R.; Li, X.; Zhen, Z.; Xu, Z.; Li, N.; He, L.; Zhu, H. A Bubble Derived Strategy to Prepare Multiple Graphene Based Porous Materials. *Adv. Funct. Mater.* **2018**, *28*, 1705879.
(28) Mu, C.; Li, J.; Song, Y.; Huang, W.; Ran, A.; Deng, K.; Huang, J.; Xie, W.; Sun, R.; Zhang, H. Enhanced Piezocapacitive Effect in Cacu3ti4o12−Polydimethylsiloxane Composited Sponge for Ultrasensitive Flexible Capacitive Sensor. *ACS Applied Nano Materials* **2018**, *1*, 274−283.
(29) Kwon, D.; Lee, T.-I.; Shim, J.; Ryu, S.; Kim, M. S.; Kim, S.; Kim, T.-S.; Park, I. Highly Sensitive, Flexible, and Wearable Pressure Sensor Based on a Giant Piezocapacitive Effect of Three-Dimensional Microporous Elastomeric Dielectric Layer. *ACS Appl. Mater. Interfaces* **2016**, *8*, 16922−16931.
(30) Kang, M.; Kim, J.; Jang, B.; Chae, Y.; Kim, J.-H.; Ahn, J.-H. Graphene-Based Three-Dimensional Capacitive Touch Sensor for Wearable Electronics. *ACS Nano* **2017**, *11*, 7950−7957.
(31) Chen, X.; Shao, J.; An, N.; Li, X.; Tian, H.; Xu, C.; Ding, Y. Self-Powered Flexible Pressure Sensors with Vertically Well-Aligned Piezoelectric Nanowire Arrays for Monitoring Vital Signs. *J. Mater. Chem. C* **2015**, *3*, 11806−11814.
(32) Pu, X.; Liu, M.; Chen, X.; Sun, J.; Du, C.; Zhang, Y.; Zhai, J.; Hu, W.; Wang, Z. L. Ultrastretchable, Transparent Triboelectric Nanogenerator as Electronic Skin for Biomechanical Energy Harvesting and Tactile Sensing. *Science Advances* **2017**, *3*, e1700015.
(33) Dahiya, A. S.; Francois, M.; Sarah, B.; Kevin, N.; Daniel, A.; Guylaine, P. V. Organic/Inorganic Hybrid Stretchable Piezoelectric Nanogenerators for Self Powered Wearable Electronics. *Advanced Materials Technologies* **2018**, *3*, 1700249.
(34) Liu, H.; Dong, M.; Huang, W.; Gao, J.; Dai, K.; Guo, J.; Zheng, G.; Liu, C.; Shen, C.; Guo, Z. Lightweight Conductive Graphene/Thermoplastic Polyurethane Foams with Ultrahigh Compressibility for Piezoresistive Sensing. *J. Mater. Chem. C* **2017**, *5*, 73−83.
(35) Hou, C.; Wang, H.; Zhang, Q.; Li, Y.; Zhu, M. Highly Conductive, Flexible, and Compressible All Graphene Passive Electronic Skin for Sensing Human Touch. *Adv. Mater.* **2014**, *26*, 5018−5024.
(36) Ma, Z.; Wei, A.; Ma, J.; Shao, L.; Jiang, H.; Dong, D.; Ji, Z.; Wang, Q.; Kang, S. Lightweight, Compressible and Electrically Conductive Polyurethane Sponges Coated with Synergistic Multiwalled Carbon Nanotubes and Graphene for Piezoresistive Sensors. *Nanoscale* **2018**, *10*, 7116−7126.
(37) Qiu, L.; Coskun, M. B.; Tang, Y.; Liu, J. Z.; Alan, T.; Ding, J.; Truong, V. T.; Li, D. Ultrafast Dynamic Piezoresistive Response of Graphene Based Cellular Elastomers. *Adv. Mater.* **2016**, *28*, 194−200.
(38) Lv, L.; Zhang, P.; Xu, T.; Qu, L. Ultrasensitive Pressure Sensor Based on an Ultralight Sparkling Graphene Block. *ACS Appl. Mater. Interfaces* **2017**, *9*, 22885−22892.
(39) Dong, X.; Wei, Y.; Chen, S.; Lin, Y.; Liu, L.; Li, J. A Linear and Large-Range Pressure Sensor Based on a Graphene/Silver Nanowires Nanobiocomposites Network and a Hierarchical Structural Sponge. *Compos. Sci. Technol.* **2018**, *155*, 108−116.
(40) Zang, X.; Wang, X.; Yang, Z.; Wang, X.; Li, R.; Chen, J.; Ji, J.; Xue, M. Unprecedented Sensitivity Towards Pressure Enabled by Graphene Foam. *Nanoscale* **2017**, *9*, 19346−19352.
(41) Wang, X.; Liu, Z.; Zhang, T. Flexible Sensing Electronics for Wearable/Attachable Health Monitoring. *Small* **2017**, *13*, 1602790.
(42) Barlian, A. A.; Park, W. T.; Mallon, J. R.; Rastegar, A. J.; Pruitt, B. L. Review: Semiconductor Piezoresistance for Microsystems. *Proc. IEEE* **2009**, *97*, 513−552.
(43) Abels, C.; Mastronardi, V.; Guido, F.; Dattoma, T.; Qualtieri, A.; Megill, W.; De Vittorio, M.; Rizzi, F. Nitride-Based Materials for Flexible Mems Tactile and Flow Sensors in Robotics. *Sensors* **2017**, *17*, 1080.
(44) Song, J.; Jiang, H.; Huang, Y.; Rogers, J. A. Mechanics of Stretchable Inorganic Electronic Materials. *J. Vac. Sci. Technol., A* **2009**, *27*, 1107−1125.
(45) Sun, Y.; Rogers, J. A. Inorganic Semiconductors for Flexible Electronics. *Adv. Mater.* **2007**, *19*, 1897−1916.
(46) Won, S. M.; Kim, H.-S.; Lu, N.; Kim, D.-G.; Solar, C. D.; Duenas, T.; Ameen, A.; Rogers, J. A. Piezoresistive Strain Sensors and Multiplexed Arrays Using Assemblies of Single-Crystalline Silicon Nanoribbons on Plastic Substrates. *IEEE Trans. Electron Devices* **2011**, *58*, 4074−4078.
(47) Rogers, J. A. Materials for Semiconductor Devices That Can Bend, Fold, Twist, and Stretch. *MRS Bull.* **2014**, *39*, 549−556.
(48) Chang, H.; Kim, S.; Jin, S.; Li, S.-W.; Yang, G.-T.; Lee, K.-Y.; Yi, H. Ultrasensitive and Highly Stable Resistive Pressure Sensors with Biomaterial-Incorporated Interfacial Layers for Wearable Health-Monitoring and Human−Machine Interfaces. *ACS Appl. Mater. Interfaces* **2018**, *10*, 1067−1076.
(49) Sun, Q.-J.; Zhuang, J.; Venkatesh, S.; Zhou, Y.; Han, S.-T.; Wu, W.; Kong, K.-W.; Li, W.-J.; Chen, X.; Li, R. K. Y.; Roy, V. A. L. Highly Sensitive and Ultrastable Skin Sensors for Biopressure and Bioforce Measurements Based on Hierarchical Microstructures. *ACS Appl. Mater. Interfaces* **2018**, *10*, 4086−4094.
(50) Huang, G.; Li, N.; Xiao, H.; Feng, Q.; Fu, S. A Paper-Based Touch Sensor with an Embedded Micro-Probe Array Fabricated by Double-Sided Laser Printing. *Nanoscale* **2017**, *9*, 9598−9605.
(51) Chen, W.; Gui, X.; Liang, B.; Yang, R.; Zheng, Y.; Zhao, C.; Li, X.; Zhu, H.; Tang, Z. Structural Engineering for High Sensitivity, Ultrathin Pressure Sensors Based on Wrinkled Graphene and Anodic Aluminum Oxide Membrane. *ACS Appl. Mater. Interfaces* **2017**, *9*, 24111−24117.
(52) Zhang, Y.; Hu, Y.; Zhu, P.; Han, F.; Zhu, Y.; Sun, R.; Wong, C.-P. Flexible and Highly Sensitive Pressure Sensor Based on Microdome-Patterned PDMS Forming with Assistance of Colloid Self-Assembly and Replica Technique for Wearable Electronics. *ACS Appl. Mater. Interfaces* **2017**, *9*, 35968−35976.
(53) Choong, C.-L.; Lee, B.-S.; Jeon, S.; Ko, D.-S.; Kang, T.-H.; Bae, J.; Lee, S. H.; Byun, K.-E.; Im, J.; Jeong, Y. J.; Park, C. E.; Park, J.-J.; Chung, U.-I. Highly Stretchable Resistive Pressure Sensors Using a Conductive Elastomeric Composite on a Micropyramid Array. *Adv. Mater.* **2014**, *26*, 3451−3458.
(54) Wang, H.; Lu, W.; Di, J.; Li, D.; Zhang, X.; Li, M.; Zhang, Z.; Zheng, L.; Li, Q. Ultra Lightweight and Highly Adaptive All Carbon Elastic Conductors with Stable Electrical Resistance. *Adv. Funct. Mater.* **2017**, *27*, 1606220.
(55) Qiu, L.; Liu, J. Z.; Chang, S. L. Y.; Wu, Y.; Li, D. Biomimetic Superelastic Graphene-Based Cellular Monoliths. *Nat. Commun.* **2012**, *3*, 1241.
(56) Xu, X.; Wang, R.; Nie, P.; Cheng, Y.; Lu, X.; Shi, L.; Sun, J. Copper Nanowire-Based Aerogel with Tunable Pore Structure and Its Application as Flexible Pressure Sensor. *ACS Appl. Mater. Interfaces* **2017**, *9*, 14273−14280.
(57) Lu, Y.; He, W.; Cao, T.; Guo, H.; Zhang, Y.; Li, Q.; Shao, Z.; Cui, Y.; Zhang, X. Elastic, Conductive, Polymeric Hydrogels and Sponges. *Sci. Rep.* **2015**, *4*, 5792.
(58) Wu, X.; Han, Y.; Zhang, X.; Zhou, Z.; Lu, C. Large Area Compliant, Low Cost, and Versatile Pressure Sensing Platform Based on Microcrack Designed Carbon Black@Polyurethane Sponge for Human−Machine Interfacing. *Adv. Funct. Mater.* **2016**, *26*, 6246−6256.
(59) Wu, Y.-h.; Liu, H.-z.; Chen, S.; Dong, X.-c.; Wang, P.-p.; Liu, S.-q.; Lin, Y.; Wei, Y.; Liu, L. Channel Crack-Designed Gold@Pu Sponge for Highly Elastic Piezoresistive Sensor with Excellent Detectability. *ACS Appl. Mater. Interfaces* **2017**, *9*, 20098−20105.
(60) Tewari, A.; Gandla, S.; Bohm, S.; McNeill, C. R.; Gupta, D. Highly Exfoliated Mwnt−Rgo Ink-Wrapped Polyurethane Foam for

DOI: 10.1021/acsami.8b20929
ACS Appl. Mater. Interfaces 2019, 11, 6685−6704

Piezoresistive Pressure Sensor Applications. *ACS Appl. Mater. Interfaces* **2018**, *10*, 5185−5195.
(61) Xue, J.; Chen, J.; Song, J.; Xu, L.; Zeng, H. Wearable and Visual Pressure Sensors Based on Zn2geo4@Polypyrrole Nanowire Aerogels. *J. Mater. Chem. C* **2017**, *5*, 11018−11024.
(62) Wang, F.; Wang, Y.; Zhan, W.; Yu, S.; Zhong, W.; Sui, G.; Yang, X. Facile Synthesis of Ultra-Light Graphene Aerogels with Super Absorption Capability for Organic Solvents and Strain-Sensitive Electrical Conductivity. *Chem. Eng. J.* **2017**, *320*, 539−548.
(63) Chen, C.; Song, J.; Zhu, S.; Li, Y.; Kuang, Y.; Wan, J.; Kirsch, D.; Xu, L.; Wang, Y.; Gao, T.; Wang, Y.; Huang, H.; Gan, W.; Gong, A.; Li, T.; Xie, J.; Hu, L. Scalable and Sustainable Approach toward Highly Compressible, Anisotropic, Lamellar Carbon Sponge. *Chem.* **2018**, *4*, 544−554.
(64) Cai, Y.; Shen, J.; Dai, Z.; Zang, X.; Dong, Q.; Guan, G.; Li, L. J.; Huang, W.; Dong, X. Extraordinarily Stretchable All Carbon Collaborative Nanoarchitectures for Epidermal Sensors. *Adv. Mater.* **2017**, *29*, 1606411.
(65) Xu, T.; Ding, Y.; Wang, Z.; Zhao, Y.; Wu, W.; Fong, H.; Zhu, Z. Three-Dimensional and Ultralight Sponges with Tunable Conductivity Assembled from Electrospun Nanofibers for a Highly Sensitive Tactile Pressure Sensor. *J. Mater. Chem. C* **2017**, *5*, 10288−10294.
(66) Yu, X.-G.; Li, Y.-Q.; Zhu, W.-B.; Huang, P.; Wang, T.-T.; Hu, N.; Fu, S.-Y. A Wearable Strain Sensor Based on a Carbonized Nano-Sponge/Silicone Composite for Human Motion Detection. *Nanoscale* **2017**, *9*, 6680−6685.
(67) Huang, W.; Dai, K.; Zhai, Y.; Liu, H.; Zhan, P.; Gao, J.; Zheng, G.; Liu, C.; Shen, C. Flexible and Lightweight Pressure Sensor Based on Carbon Nanotube/Thermoplastic Polyurethane-Aligned Conductive Foam with Superior Compressibility and Stability. *ACS Appl. Mater. Interfaces* **2017**, *9*, 42266−42277.
(68) Wang, C.; Ding, Y.; Yuan, Y.; Cao, A.; He, X.; Peng, Q.; Li, Y. Multifunctional, Highly Flexible, Free Standing 3D Polypyrrole Foam. *Small* **2016**, *12*, 4070−4076.
(69) Zhao, X.-H.; Ma, S.-N.; Long, H.; Yuan, H.; Tang, C. Y.; Cheng, P. K.; Tsang, Y. H. Multifunctional Sensor Based on Porous Carbon Derived from Metal−Organic Frameworks for Real Time Health Monitoring. *ACS Appl. Mater. Interfaces* **2018**, *10*, 3986−3993.
(70) Pang, Y.; Tian, H.; Tao, L.; Li, Y.; Wang, X.; Deng, N.; Yang, Y.; Ren, T.-L. Flexible, Highly Sensitive, and Wearable Pressure and Strain Sensors with Graphene Porous Network Structure. *ACS Appl. Mater. Interfaces* **2016**, *8*, 26458−26462.
(71) Cai, Y.; Shen, J.; Dai, Z.; Zang, X.; Dong, Q.; Guan, G.; Li, L. J.; Huang, W.; Dong, X. Extraordinarily Stretchable All Carbon Collaborative Nanoarchitectures for Epidermal Sensors. *Adv. Mater.* **2017**, *29*, 1606411.
(72) Luo, Y.; Xiao, Q.; Li, B. Highly Compressible Graphene/Polyurethane Sponge with Linear and Dynamic Piezoresistive Behavior. *RSC Adv.* **2017**, *7*, 34939−34944.
(73) Liang, S.; Li, Y.; Yang, J.; Zhang, J.; He, C.; Liu, Y.; Zhou, X. 3D Stretchable, Compressible, and Highly Conductive Metal Coated Polydimethylsiloxane Sponges. *Advanced Materials Technologies* **2016**, *1*, 1600117.
(74) Yao, H. B.; Ge, J.; Wang, C. F.; Wang, X.; Hu, W.; Zheng, Z. J.; Ni, Y.; Yu, S. H. A Flexible and Highly Pressure Sensitive Graphene−Polyurethane Sponge Based on Fractured Microstructure Design. *Adv. Mater.* **2013**, *25*, 6692−6698.
(75) Kuang, J.; Liu, L.; Gao, Y.; Zhou, D.; Chen, Z.; Han, B.; Zhang, Z. A Hierarchically Structured Graphene Foam and Its Potential as a Large-Scale Strain-Gauge Sensor. *Nanoscale* **2013**, *5*, 12171−12177.
(76) Liu, W.; Liu, N.; Yue, Y.; Rao, J.; Luo, C.; Zhang, H.; Yang, C.; Su, J.; Liu, Z.; Gao, Y. A Flexible and Highly Sensitive Pressure Sensor Based on Elastic Carbon Foam. *J. Mater. Chem. C* **2018**, *6*, 1451−1458.
(77) Wu, Z. Y.; Li, C.; Liang, H. W.; Chen, J. F.; Yu, S. H. Ultralight, Flexible, and Fire Resistant Carbon Nanofiber Aerogels from Bacterial Cellulose. *Angew. Chem.* **2013**, *125*, 2997−3001.
(78) Zhao, S.; Zhang, G.; Gao, Y.; Deng, L.; Li, J.; Sun, R.; Wong, C.-P. Strain-Driven and Ultrasensitive Resistive Sensor/Switch Based on Conductive Alginate/Nitrogen-Doped Carbon-Nanotube-Supported Ag Hybrid Aerogels with Pyramid Design. *ACS Appl. Mater. Interfaces* **2014**, *6*, 22823−22829.
(79) Hou, Y.; Wang, D.; Zhang, X.-M.; Zhao, H.; Zha, J.-W.; Dang, Z.-M. Positive Piezoresistive Behavior of Electrically Conductive Alkyl-Functionalized Graphene/Polydimethylsilicone Nanocomposites. *J. Mater. Chem. C* **2013**, *1*, 515−521.
(80) Tung, T. T.; Robert, C.; Castro, M.; Feller, J. F.; Kim, T. Y.; Suh, K. S. Enhancing the Sensitivity of Graphene/Polyurethane Nanocomposite Flexible Piezo-Resistive Pressure Sensors with Magnetite Nano-Spacers. *Carbon* **2016**, *108*, 450−460.
(81) Luo, N.; Huang, Y.; Liu, J.; Chen, S. C.; Wong, C. P.; Zhao, N. Hollow Structured Graphene−Silicone Composite Based Piezoresistive Sensors: Decoupled Property Tuning and Bending Reliability. *Adv. Mater.* **2017**, *29*, 1702675.
(82) Huang, J.; Wang, J.; Yang, Z.; Yang, S. High-Performance Graphene Sponges Reinforced with Polyimide for Room-Temperature Piezoresistive Sensing. *ACS Appl. Mater. Interfaces* **2018**, *10*, 8180−8189.
(83) Liu, X.; Tang, C.; Du, X.; Xiong, S.; Xi, S.; Liu, Y.; Shen, X.; Zheng, Q.; Wang, Z.; Wu, Y.; Horner, A.; Kim, J.-K. A Highly Sensitive Graphene Woven Fabric Strain Sensor for Wearable Wireless Musical Instruments. *Mater. Horiz.* **2017**, *4*, 477−486.
(84) Zheng, Q.; Liu, X.; Xu, H.; Cheung, M.-S.; Choi, Y.-W.; Huang, H.-C.; Lei, H.-Y.; Shen, X.; Wang, Z.; Wu, Y.; Kim, S. Y.; Kim, J.-K. Sliced Graphene Foam Films for Dual-Functional Wearable Strain Sensors and Switches. *Nanoscale Horiz.* **2018**, *3*, 35−44.
(85) Yang, C.; Xu, Y.; Man, P.; Zhang, H.; Huo, Y.; Yang, C.; Li, Z.; Jiang, S.; Man, B. Formation of Large-Area Stretchable 3D Graphene-Nickel Particle Foams and Their Sensor Applications. *RSC Adv.* **2017**, *7*, 35016−35026.
(86) Brady, S.; Diamond, D.; Lau, K.-T. Inherently Conducting Polymer Modified Polyurethane Smart Foam for Pressure Sensing. *Sens. Actuators, A* **2005**, *119*, 398−404.
(87) Langner, M.; Agarwal, S.; Baudler, A.; Schröder, U.; Greiner, A. Large Multipurpose Exceptionally Conductive Polymer Sponges Obtained by Efficient Wet Chemical Metallization. *Adv. Funct. Mater.* **2015**, *25*, 6182−6188.
(88) Chun, S.; Hong, A.; Choi, Y.; Ha, C.; Park, W. A Tactile Sensor Using a Conductive Graphene-Sponge Composite. *Nanoscale* **2016**, *8*, 9185−9192.
(89) Zhang, H.; Liu, N.; Shi, Y.; Liu, W.; Yue, Y.; Wang, S.; Ma, Y.; Wen, L.; Li, L.; Long, F.; Zou, Z.; Gao, Y. Piezoresistive Sensor with High Elasticity Based on 3D Hybrid Network of Sponge@CNTs@Ag Nps. *ACS Appl. Mater. Interfaces* **2016**, *8*, 22374−22381.
(90) Iglio, R.; Mariani, S.; Robbiano, V.; Strambini, L.; Barillaro, G. Flexible Polydimethylsiloxane Foams Decorated with Multiwalled Carbon Nanotubes Enable Unprecedented Detection of Ultralow Strain and Pressure Coupled with a Large Working Range. *ACS Appl. Mater. Interfaces* **2018**, *10*, 13877−13885.
(91) Zhang, B.-X.; Hou, Z.-L.; Yan, W.; Zhao, Q.-L.; Zhan, K.-T. Multi-Dimensional Flexible Reduced Graphene Oxide/Polymer Sponges for Multiple Forms of Strain Sensors. *Carbon* **2017**, *125*, 199−206.
(92) Cheng, H.; Du, Y.; Wang, B.; Mao, Z.; Xu, H.; Zhang, L.; Zhong, Y.; Jiang, W.; Wang, L.; Sui, X. Flexible Cellulose-Based Thermoelectric Sponge Towards Wearable Pressure Sensor and Energy Harvesting. *Chem. Eng. J.* **2018**, *338*, 1−7.
(93) Luo, M.; Li, M.; Li, Y.; Chang, K.; Liu, K.; Liu, Q.; Wang, Y.; Lu, Z.; Liu, X.; Wang, D. In-Situ Polymerization of Ppy/Cellulose Composite Sponge with High Elasticity and Conductivity for the Application of Pressure Sensor. *Composites Communications* **2017**, *6*, 68−72.
(94) Dong, X.-C.; Ge, G.; Cai, Y.; Dong, Q.; Zhang, Y.; Shao, J.; Huang, W. Flexible Pressure Sensor Based on Rgo/Polyaniline Wrapped Sponge with Tunable Sensitivity for Human Motions Detection. *Nanoscale* **2018**, *10*, 10033.
(95) Chen, Z.; Ren, W.; Gao, L.; Liu, B.; Pei, S.; Cheng, H.-M. Three-Dimensional Flexible and Conductive Interconnected Gra-

DOI: 10.1021/acsami.8b20929
ACS Appl. Mater. Interfaces 2019, 11, 6685−6704

phene Networks Grown by Chemical Vapour Deposition. *Nat. Mater.* **2011**, *10*, 424.
(96) Xu, Y.; Sheng, K.; Li, C.; Shi, G. Self-Assembled Graphene Hydrogel Via a One-Step Hydrothermal Process. *ACS Nano* **2010**, *4*, 4324−4330.
(97) Nardecchia, S.; Carriazo, D.; Ferrer, M. L.; Gutierrez, M. C.; del Monte, F. Three Dimensional Macroporous Architectures and Aerogels Built of Carbon Nanotubes and/or Graphene: Synthesis and Applications. *Chem. Soc. Rev.* **2013**, *42*, 794−830.
(98) Mao, J.; Iocozzia, J.; Huang, J.; Meng, K.; Lai, Y.; Lin, Z. Graphene Aerogels for Efficient Energy Storage and Conversion. *Energy Environ. Sci.* **2018**, *11*, 772−799.
(99) Moon, I. K.; Yoon, S.; Chun, K. Y.; Oh, J. Highly Elastic and Conductive N Doped Monolithic Graphene Aerogels for Multifunctional Applications. *Adv. Funct. Mater.* **2015**, *25*, 6976−6984.
(100) Jiang, S.; Agarwal, S.; Greiner, A. Low Density Open Cellular Sponges as Functional Materials. *Angew. Chem., Int. Ed.* **2017**, *56*, 15520−15538.
(101) Zhu, D.; Handschuh-Wang, S.; Zhou, X. Recent Progress in Fabrication and Application of Polydimethylsiloxane Sponges. *J. Mater. Chem. A* **2017**, *5*, 16467−16497.
(102) Deville, S.; Saiz, E.; Nalla, R. K.; Tomsia, A. P. Freezing as a Path to Build Complex Composites. *Science* **2006**, *311*, 515−518.
(103) Coskun, M. B.; Qiu, L.; Arefin, M. S.; Neild, A.; Yuce, M.; Li, D.; Alan, T. Detecting Subtle Vibrations Using Graphene-Based Cellular Elastomers. *ACS Appl. Mater. Interfaces* **2017**, *9*, 11345−11349.
(104) Tsui, M. N.; Islam, M. F. Creep- and Fatigue-Resistant, Rapid Piezoresistive Responses of Elastomeric Graphene-Coated Carbon Nanotube Aerogels over a Wide Pressure Range. *Nanoscale* **2017**, *9*, 1128−1135.
(105) Lv, P.; Yu, K.; Tan, X.; Zheng, R.; Ni, Y.; Wang, Z.; Liu, C.; Wei, W. Super-Elastic Graphene/Carbon Nanotube Aerogels and Their Application as a Strain-Gauge Sensor. *RSC Adv.* **2016**, *6*, 11256−11261.
(106) Ma, Y.; Yue, Y.; Zhang, H.; Cheng, F.; Zhao, W.; Rao, J.; Luo, S.; Wang, J.; Jiang, X.; Liu, Z.; Liu, N.; Gao, Y. 3D Synergistical Mxene/Reduced Graphene Oxide Aerogel for a Piezoresistive Sensor. *ACS Nano* **2018**, *12*, 3209−3216.
(107) Zuruzi, A. S.; Haffiz, T. M.; Affidah, D.; Amirul, A.; Norfatriah, A.; Nurmawati, M. H. Towards Wearable Pressure Sensors Using Multiwall Carbon Nanotube/Polydimethylsiloxane Nanocomposite Foams. *Mater. Des.* **2017**, *132*, 449−458.
(108) Yang, L.; Wang, R.; Song, Q.; Liu, Y.; Zhao, Q.; Shen, Y. One-Pot Preparation of Porous Piezoresistive Sensor with High Strain Sensitivity Via Emulsion-Templated Polymerization. *Composites, Part A* **2017**, *101*, 195−198.
(109) Xiao, J.; Tan, Y.; Song, Y.; Zheng, Q. A Flyweight and Superelastic Graphene Aerogel as a High-Capacity Adsorbent and Highly Sensitive Pressure Sensor. *J. Mater. Chem. A* **2018**, *6*, 9074−9080.
(110) Guo, C.; Kondo, Y.; Takai, C.; Fuji, M. Multi-Walled Carbon Nanotubes/Silicone Conductive Foams and Their Piezoresistive Behaviors. *J. Mater. Sci.: Mater. Electron.* **2017**, *28*, 7633−7642.
(111) Ding, Y.; Hou, H.; Zhao, Y.; Zhu, Z.; Fong, H. Electrospun Polyimide Nanofibers and Their Applications. *Prog. Polym. Sci.* **2016**, *61*, 67−103.
(112) Qin, Y.; Peng, Q.; Ding, Y.; Lin, Z.; Wang, C.; Li, Y.; Xu, F.; Li, J.; Yuan, Y.; He, X.; Li, Y. Lightweight, Superelastic, and Mechanically Flexible Graphene/Polyimide Nanocomposite Foam for Strain Sensor Application. *ACS Nano* **2015**, *9*, 8933−8941.
(113) Wang, M.; Anoshkin, I. V.; Nasibulin, A. G.; Korhonen, J. T.; Seitsonen, J.; Pere, J.; Kauppinen, E. I.; Ras, R. H. A.; Ikkala, O. Modifying Native Nanocellulose Aerogels with Carbon Nanotubes for Mechanoresponsive Conductivity and Pressure Sensing. *Adv. Mater.* **2013**, *25*, 2428−2432.
(114) Hosseini, H.; Kokabi, M.; Mousavi, S. M. Bc/Rgo Conductive Nanocomposite Aerogel as a Strain Sensor. *Polymer* **2018**, *137*, 82−96.
(115) Si, Y.; Yu, J.; Tang, X.; Ge, J.; Ding, B. Ultralight Nanofibre-Assembled Cellular Aerogels with Superelasticity and Multifunctionality. *Nat. Commun.* **2014**, *5*, 5802.
(116) Si, Y.; Fu, Q.; Wang, X.; Zhu, J.; Yu, J.; Sun, G.; Ding, B. Superelastic and Superhydrophobic Nanofiber-Assembled Cellular Aerogels for Effective Separation of Oil/Water Emulsions. *ACS Nano* **2015**, *9*, 3791−3799.
(117) Si, Y.; Wang, X.; Dou, L.; Yu, J.; Ding, B. Ultralight and Fire-Resistant Ceramic Nanofibrous Aerogels with Temperature-Invariant Superelasticity. *Sci. Adv.* **2018**, *4*, No. eaas8925.
(118) Duan, G.; Jiang, S.; Jérôme, V.; Wendorff, J. H.; Fathi, A.; Uhm, J.; Altstädt, V.; Herling, M.; Breu, J.; Freitag, R.; Agarwal, S.; Greiner, A. Ultralight, Soft Polymer Sponges by Self Assembly of Short Electrospun Fibers in Colloidal Dispersions. *Adv. Funct. Mater.* **2015**, *25*, 2850−2856.
(119) Xu, T.; Miszuk, J. M.; Zhao, Y.; Sun, H.; Fong, H. Electrospun Polycaprolactone 3D Nanofibrous Scaffold with Interconnected and Hierarchically Structured Pores for Bone Tissue Engineering. *Adv. Healthcare Mater.* **2015**, *4*, 2238−2246.
(120) Xu, T.; Wang, Z.; Ding, Y.; Xu, W.; Wu, W.; Zhu, Z.; Fong, H. Ultralight Electrospun Cellulose Sponge with Super-High Capacity on Absorption of Organic Compounds. *Carbohydr. Polym.* **2018**, *179*, 164−172.
(121) Lai, F.; Huang, Y.; Zuo, L.; Gu, H.; Miao, Y.-E.; Liu, T. Electrospun Nanofiber-Supported Carbon Aerogel as a Versatile Platform toward Asymmetric Supercapacitors. *J. Mater. Chem. A* **2016**, *4*, 15861−15869.
(122) Si, Y.; Wang, X.; Yan, C.; Yang, L.; Yu, J.; Ding, B. Ultralight Biomass Derived Carbonaceous Nanofibrous Aerogels with Superelasticity and High Pressure Sensitivity. *Adv. Mater.* **2016**, *28*, 9512−9518.
(123) Kim, C.; Cho, Y. J.; Yun, W. Y.; Ngoc, B. T. N.; Yang, K. S.; Chang, D. R.; Lee, J. W.; Kojima, M.; Kim, Y. A.; Endo, M. Fabrications and Structural Characterization of Ultra-Fine Carbon Fibres by Electrospinning of Polymer Blends. *Solid State Commun.* **2007**, *142*, 20−23.
(124) Chen, S.; He, G.; Hu, H.; Jin, S.; Zhou, Y.; He, Y.; He, S.; Zhao, F.; Hou, H. Elastic Carbon Foam Via Direct Carbonization of Polymer Foam for Flexible Electrodes and Organic Chemical Absorption. *Energy Environ. Sci.* **2013**, *6*, 2435−2439.
(125) Zhang, H.; Zhou, Y.; Li, C.; Chen, S.; Liu, L.; Liu, S.; Yao, H.; Hou, H. Porous Nitrogen Doped Carbon Foam with Excellent Resilience for Self-Supported Oxygen Reduction Catalyst. *Carbon* **2015**, *95*, 388−395.
(126) Wang, Z.; Jiang, R.; Li, G.; Chen, Y.; Tang, Z.; Wang, Y.; Liu, Z.; Jiang, H.; Zhi, C. Flexible Dual-Mode Tactile Sensor Derived from Three-Dimensional Porous Carbon Architecture. *ACS Appl. Mater. Interfaces* **2017**, *9*, 22685−22693.
(127) Chen, Y.; Sheng, C.; Dang, B.; Qian, T.; Jin, C.; Sun, Q. High Mechanical Property of Laminated Electromechanical Sensors by Carbonized Nanolignocellulose/Graphene Composites. *ACS Appl. Mater. Interfaces* **2018**, *10*, 7344−7351.
(128) Zhuo, H.; Hu, Y.; Tong, X.; Chen, Z.; Zhong, L.; Lai, H.; Liu, L.; Jing, S.; Liu, Q.; Liu, C.; Peng, X.; Sun, R. A Supercompressible, Elastic, and Bendable Carbon Aerogel with Ultrasensitive Detection Limits for Compression Strain, Pressure, and Bending Angle. *Adv. Mater.* **2018**, *30*, 1706705.
(129) Song, J.; Chen, C.; Yang, Z.; Kuang, Y.; Li, T.; Li, Y.; Huang, H.; Kierzewski, I.; Liu, B.; He, S.; Gao, T.; Yuruker, S. U.; Gong, A.; Yang, B.; Hu, L. Highly Compressible, Anisotropic Aerogel with Aligned Cellulose Nanofibers. *ACS Nano* **2018**, *12*, 140−147.
(130) Wu, S.; Zhang, J.; Ladani, R. B.; Ravindran, A. R.; Mouritz, A. P.; Kinloch, A. J.; Wang, C. H. Novel Electrically Conductive Porous PDMS/Carbon Nanofiber Composites for Deformable Strain Sensors and Conductors. *ACS Appl. Mater. Interfaces* **2017**, *9*, 14207−14215.
(131) Cho, D.; Park, J.; Kim, J.; Kim, T.; Kim, J.; Park, I.; Jeon, S. Three-Dimensional Continuous Conductive Nanostructure for Highly Sensitive and Stretchable Strain Sensor. *ACS Appl. Mater. Interfaces* **2017**, *9*, 17369−17378.

DOI: 10.1021/acsami.8b20929
ACS Appl. Mater. Interfaces 2019, 11, 6685−6704

(132) Zhu, J.; Ding, Y.; Agarwal, S.; Greiner, A.; Zhang, H.; Hou, H. Nanofibre Preparation of Non-Processable Polymers by Solid-State Polymerization of Molecularly Self-Assembled Monomers. *Nanoscale* **2017**, *9*, 18169−18174.
(133) Samad, Y. A.; Li, Y.; Schiffer, A.; Alhassan, S. M.; Liao, K. Graphene Foam Developed with a Novel Two Step Technique for Low and High Strains and Pressure Sensing Applications. *Small* **2015**, *11*, 2380−2385.
(134) Ma, Y.; Yu, M.; Liu, J.; Li, X.; Li, S. Ultralight Interconnected Graphene−Amorphous Carbon Hierarchical Foam with Mechanical Resiliency for High Sensitivity and Durable Strain Sensors. *ACS Appl. Mater. Interfaces* **2017**, *9*, 27127−27134.
(135) Liu, W.; Chen, Z.; Zhou, G.; Sun, Y.; Lee, H. R.; Liu, C.; Yao, H.; Bao, Z.; Cui, Y. 3D Porous Sponge Inspired Electrode for Stretchable Lithium Ion Batteries. *Adv. Mater.* **2016**, *28*, 3578−3583.
(136) Chen, H.; Miao, L.; Su, Z.; Song, Y.; Han, M.; Chen, X.; Cheng, X.; Chen, D.; Zhang, H. Fingertip-Inspired Electronic Skin Based on Triboelectric Sliding Sensing and Porous Piezoresistive Pressure Detection. *Nano Energy* **2017**, *40*, 65−72.
(137) Rinaldi, A.; Tamburrano, A.; Fortunato, M.; Sarto, M. A Flexible and Highly Sensitive Pressure Sensor Based on a PDMS Foam Coated with Graphene Nanoplatelets. *Sensors* **2016**, *16*, 2148.
(138) Li, C.; Jiang, D.; Liang, H.; Huo, B.; Liu, C.; Yang, W.; Liu, J. Superelastic and Arbitrary Shaped Graphene Aerogels with Sacrificial Skeleton of Melamine Foam for Varied Applications. *Adv. Funct. Mater.* **2018**, *28*, 1704674.
(139) Dai, Z.; Weng, C.; Liu, L.; Hou, Y.; Zhao, X.; Kuang, J.; Shi, J.; Wei, Y.; Lou, J.; Zhang, Z. Multifunctional Polymer-Based Graphene Foams with Buckled Structure and Negative Poisson's Ratio. *Sci. Rep.* **2016**, *6*, 32989.
(140) Ugarte, L.; Gómez-Fernández, S.; Tercjak, A.; Martínez-Amesti, A.; Corcuera, M. A.; Eceiza, A. Strain Sensitive Conductive Polyurethane Foam/Graphene Nanocomposites Prepared by Impregnation Method. *Eur. Polym. J.* **2017**, *90*, 323−333.
(141) Boland, C. S.; Khan, U.; Binions, M.; Barwich, S.; Boland, J. B.; Weaire, D.; Coleman, J. N. Graphene-Coated Polymer Foams as Tuneable Impact Sensors. *Nanoscale* **2018**, *10*, 5366−5375.
(142) Gong, S.; Schwalb, W.; Wang, Y.; Chen, Y.; Tang, Y.; Si, J.; Shirinzadeh, B.; Cheng, W. A Wearable and Highly Sensitive Pressure Sensor with Ultrathin Gold Nanowires. *Nat. Commun.* **2014**, *5*, 3132.
(143) Yue, Y.; Liu, N.; Liu, W.; Li, M.; Ma, Y.; Luo, C.; Wang, S.; Rao, J.; Hu, X.; Su, J.; Zhang, Z.; Huang, Q.; Gao, Y. 3D Hybrid Porous Mxene-Sponge Network and Its Application in Piezoresistive Sensor. *Nano Energy* **2018**, *50*, 79−87.
(144) Hong, S. Y.; Oh, J. H.; Park, H.; Yun, J. Y.; Jin, S. W.; Sun, L.; Zi, G.; Ha, J. S. Polyurethane Foam Coated with a Multi-Walled Carbon Nanotube/Polyaniline Nanocomposite for a Skin-Like Stretchable Array of Multi-Functional Sensors. *NPG Asia Mater.* **2017**, *9*, No. e448.
(145) Ma, Z.; Su, B.; Gong, S.; Wang, Y.; Yap, L. W.; Simon, G. P.; Cheng, W. Liquid-Wetting-Solid Strategy to Fabricate Stretchable Sensors for Human-Motion Detection. *ACS Sens.* **2016**, *1*, 303−311.
(146) Xu, R.; Zhang, K.; Xu, X.; He, M.; Lu, F.; Su, B. Superhydrophobic Ws2 Nanosheet Wrapped Sponges for Underwater Detection of Tiny Vibration. *Adv. Sci.* **2018**, *5*, 1700655.
(147) da Silva, F. A. G.; de Araújo, C. M. S.; Alcaraz Espinoza, J. J.; de Oliveira, H. P. Toward Flexible and Antibacterial Piezoresistive Porous Devices for Wound Dressing and Motion Detectors. *J. Polym. Sci., Part B: Polym. Phys.* **2018**, *56*, 1063−1072.
(148) Yu, Y.; Zeng, J.; Chen, C.; Xie, Z.; Guo, R.; Liu, Z.; Zhou, X.; Yang, Y.; Zheng, Z. Three Dimensional Compressible and Stretchable Conductive Composites. *Adv. Mater.* **2014**, *26*, 810−815.
(149) Amjadi, M.; Pichitpajongkit, A.; Lee, S.; Ryu, S.; Park, I. Highly Stretchable and Sensitive Strain Sensor Based on Silver Nanowire−Elastomer Nanocomposite. *ACS Nano* **2014**, *8*, 5154−5163.
(150) Nagels, S.; Wim, D. Fabrication Approaches to Interconnect Based Devices for Stretchable Electronics: A Review. *Materials* **2018**, *11*, 375.
(151) Zheng, Y.-L.; Ding, X.-R.; Poon, C. C. Y.; Lo, B. P. L.; Zhang, H.; Zhou, X.-L.; Yang, G.-Z.; Zhao, N.; Zhang, Y.-T. Unobtrusive Sensing and Wearable Devices for Health Informatics. *IEEE Trans. Biomed. Eng.* **2014**, *61*, 1538−1554.
(152) Bartlett, M. D.; Markvicka, E. J.; Majidi, C. Rapid Fabrication of Soft, Multilayered Electronics for Wearable Biomonitoring. *Adv. Funct. Mater.* **2016**, *26*, 8496−8504.
(153) Garcia, C.; Trendafilova, I.; Guzman de Villoria, R.; Sanchez del Rio, J. Self-Powered Pressure Sensor Based on the Triboelectric Effect and Its Analysis Using Dynamic Mechanical Analysis. *Nano Energy* **2018**, *50*, 401−409.

DOI: 10.1021/acsami.8b20929
ACS Appl. Mater. Interfaces 2019, 11, 6685−6704